



CHARACTERIZATION AND VALORIZATION DIAGNOSIS  
OF GENERATED WASTES IN THE DECONTAMINATION  
PROCESS OF PHOSPHOGYPSUM LEACHATE

CECCOTTI RODRIGUEZ, Estefanía Inés

Trabajo entregado para la obtención del grado de **MÁSTER**  
**EN TECNOLOGÍA AMBIENTAL**

Modalidad: Investigación

Diciembre / 2022

Directores:

Dr. Manuel Jesús Gázquez González

Dra. Silvia María Pérez Moren



**D. Manuel Jesús Gázquez González**, DNI: 34073072K, Profesor titular de Universidad en el Departamento de Física Aplicada de la Universidad de Cádiz, y **Dña. Silvia María Pérez Moreno**, DNI: 44203353K, Investigadora Postdoctoral en el Departamento de Ciencias Integradas, en el Área de Física Aplicada de la Universidad de Huelva.

### **INFORMAN:**

Que el trabajo titulado “**Characterization and valorization diagnosis of generated wastes in the decontamination process of phosphogypsum leachate**” presentado por **Estefanía Ceccotti Rodríguez, con D.N.I.: AAE057021**, ha sido realizado en el grupo de Investigación FRYMA (Física, Radiaciones y Medio Ambiente) del Centro RENSMA (Centro de Investigación en Recursos Naturales, Salud y Medio Ambiente) de la Universidad de Huelva, bajo mi dirección, y autorizo su presentación y defensa como **Trabajo Fin de Máster**, Modalidad: Trabajo de Investigación para el Máster Universitario en Tecnología Ambiental de la Universidad de Huelva.

En Huelva, a 7 de Diciembre de 2022

Fdo.: Manuel Jesús Gázquez  
González

Fdo.: Silvia María Pérez  
Moreno







## RESUMEN

El interés en la producción de ácido fosfórico se centra en la obtención de fertilizantes, para dar respuesta a las demandas de la población actual en lo que respecta a la producción y el consumo de alimentos. El ácido fosfórico se obtiene por disolución de la roca fosfática con ácido sulfúrico, obteniéndose como residuo del proceso, el fosfoyeso, principalmente formado por yeso ( $\text{CaSO}_4 \cdot 2\text{H}_2\text{O}$ ). Anualmente, en el mundo se utilizan alrededor de 240 Mt de roca fosfato, las cuales producen unas 300 Mt de fosfoyeso, cuyo sistema de gestión más habitual es su almacenamiento en grandes apilamientos.

Los residuos de fosfoyeso son considerados residuos NORM (Naturally Occurring Radioactive Material) ya que sus concentraciones de radionucleidos naturales exceden los límites establecidos en la legislación y, por lo tanto, este hecho representa un problema adicional desde el punto de vista radiológico y medioambiental.

En el estudio que se desarrolla en este trabajo, se analizan los lixiviados de las balsas de fosfoyeso de la ciudad de Huelva, y se realiza una profunda caracterización fisicoquímica y radiológica de los materiales obtenidos durante las reacciones químicas producidas en su descontaminación, para posteriormente realizar un diagnóstico de las posibles opciones de valorización de los mismos.

En particular, en este trabajo se llevó a cabo un proceso de selección de neutralizantes y optimización de neutralización secuencial en dos etapas. La primera fase del proceso consiste en alcanzar un pH en torno a 3.5 y la segunda fase se lleva hasta  $\text{pH} = 12$ . Para ello, se evaluó el uso de varios agentes alcalinos, tales como  $\text{Ca}(\text{OH})_2$  y  $\text{CaCO}_3$ . Finalmente, tras el tratamiento se obtiene un efluente que cumple con todos los requisitos de concentraciones de vertido establecidos por la legislación vigente en la Comunidad de Andalucía.

En el proceso de limpieza, se obtuvieron dos residuos sólidos concretos: en la primera etapa se obtuvo fluorita, con potencial aplicación como aditivo en la fabricación del cemento y en la segunda, hidroxiapatita, cuya aplicación posible podría ser la síntesis de ácido fosfórico tan demandado para la producción de los fertilizantes. Por último, se realizó un diagnóstico de las aplicaciones concretas de dichos residuos, de manera que los resultados hallados puedan servir de antecedentes para lugares con similar problemática, ya que el objetivo principal fue neutralizar el lixiviado de fosfoyeso, obteniéndose varios residuos que podrían destinarse a diferentes aplicaciones comerciales, favoreciendo la economía circular.



## ABSTRACT

The interest in the production of phosphoric acid focuses on obtaining fertilizers, to respond to the demands of the current population in terms of food production and consumption. Phosphoric acid is obtained by diluting phosphate rock in sulfuric acid, obtaining phosphogypsum as a waste of the process, formed mainly by gypsum ( $\text{CaSO}_4 \cdot 2\text{H}_2\text{O}$ ). Annually, around 240 Mt of phosphate rock are used in the world, which produce about 300 Mt of phosphogypsum, whose most common management system is its storage in large piles.

Phosphogypsum waste is considered a NORM waste (Naturally Occurring Radioactive Material) since its concentrations of natural radionuclides exceed the limits established in the legislation, and therefore, this fact represents an additional problem from the radiological and environmental point of view.

In the study that is developed in this work, the leachate from the phosphogypsum piles of the city of Huelva is analyzed, and a depth physicochemical and radiological characterization of the wastes generated during the chemical reactions produced in its decontamination is carried out, for later making out a diagnosis of the possible waste valorization options.

In particular, an optimized two steps sequential neutralization process was conducted. The first phase of the process consists of reaching a pH of around 3.5 and the second phase is up to pH 12. For this, the use of various alkaline reagents, such as  $\text{Ca}(\text{OH})_2$  and  $\text{CaCO}_3$ , was evaluated. The reason for choosing these specific stages was due to the fact that in previous studies it was found that in the first stage, the fluorides contained in the phosphogypsum leachate precipitated, forming calcium compounds that are of special interest in their valorization and, on the other hand, in the second step, the phosphates precipitated, forming a second waste for recovery or reuse. Finally, after treatment, an effluent that complies all set out requirements for concentrations of discharge established by current legislation in the Andalusia region is obtained.

Since neutralization was carried out in two stages, two specific solid wastes were obtained. In the first stage, fluorite was obtained, with potential application in the manufacture of cement as an additive. In the second stage, hydroxyapatite was obtained, whose application could be the synthesis of phosphoric acid, which is so demanded for the production of fertilizers. Finally, a diagnosis of the specific application of the wastes was carried out, so that the results found can serve as a background for places with similar problems, since the main objective was to neutralize the phosphogypsum leachate, obtaining various wastes that could be used for different commercial applications, on favor of the circular economy.



## CONTENT

RESUMEN.....	1
ABSTRACT .....	2
1. INTRODUCTION.....	7
1.1 Environmental problem.....	10
1.2 Process and treatments of acid leachates.....	12
1.3 Circular economy.....	13
1.4 Objectives.....	14
1.4.1 General objective .....	14
1.4.2 Specific objectives .....	14
2 MATERIALS AND METHODS.....	14
2.1 Sampling .....	14
2.1 Design of experiments .....	15
2.2 Characterization techniques.....	18
2.3.1 Physicochemical techniques .....	18
2.3.1.1 Inductively coupled plasma mass spectrometry (ICP-MS).....	18
2.3.1.2 Inductively coupled plasma optical emission spectrometry (ICP-OES) .....	18
2.3.1.3 Ion Chromatography .....	19
2.3.1.4 X-Ray fluorescence (XRF) .....	20
2.3.1.5 X-Ray Diffraction (XRD).....	21
2.3.2 Radiometric techniques .....	22
2.3.2.1 Alpha spectrometry .....	22
2.3.3 Leaching test .....	23
3 RESULTS AND DISCUSSION .....	24
3.1 Physicochemical characterization of phosphogypsum leachate (PGL) .....	24
3.1 Samples characterization .....	26
3.1.1 Liquid fraction.....	27
3.1.2. Solid fraction.....	32
3.1.2 Precipitation efficiencies .....	38
3.2 Environmental Implications.....	42
3.2.1 Liquid discharge limits in Andalusia.....	42





3.2.2	Landfill disposal admission.....	44
3.3	Diagnosis of valorization for the generated wastes .....	46
3.4.1	Fluorite .....	46
3.4.2	Hydroxyapatite.....	50
4	CONCLUSIONS .....	53
5	REFERENCES.....	55
6	ANEXXES .....	61
6.1	Composition (mg/L) of PGL and liquid fraction measured by ICP-OES and ICP-MS. ....	61
6.2	Diffraction patterns of solid fraction formed after neutralization treatment measured by XRD.....	67
6.3	Mineral composition of solid fraction formed after neutralization treatment measured by XRD.....	71
6.4	Elemental composition (% and ppm) of solid fraction formed after neutralization treatment measured by ICP-MS and XRF. ....	72
6.5	Material balances - Composition of liquid and solid fraction during neutralization treatment (Process A .....	75
6.6	Material balances - Composition of liquid and solid fraction during neutralization treatment (Process B).....	76
6.7	Element precipitation percentage during process A and B.....	76
6.8	Composition of reagents used in sequential optimization neutralization process, A and B – measured by ICP-MS.....	78



## List of figures

Figure 1: Location of the city, Industrial Complex and the PG stacks.....	9
Figure 2: Leachate from the perimeter channel.....	11
Figure 3: Location of sampling area. ....	15
Figure 4: Diagram of sequential neutralization process A .....	17
Figure 5: Diagram of sequential neutralization process B .....	17
Figure 6: Concentration of main elements in liquid fraction in process A. ....	28
Figure 7: Concentration of minor elements in liquid fraction in process A. ....	28
Figure 8: Concentration of main elements in liquid fraction in process B. ....	29
Figure 9: Concentration of minor elements in liquid fraction in process B. ....	30
Figure 10: Anion concentration (mg/L) of PGL and liquid fraction measured by ion chromatography.....	31
Figure 11: Elemental composition (%) of main elements in solids from process A. ....	33
Figure 12: Elemental composition (%) of main elements in solids from process B. ....	33
Figure 13: Elemental composition (ppm) of minor elements in solids obtained in process A.....	34
Figure 14: Elemental composition (ppm) of minor elements in solids obtained in process B.....	34
Figure 15: Mineral composition of solid fraction formed after neutralization treatment measured by XRD. ....	36
Figure 16: Scheme of fractions obtained in the experiments. ....	39
Figure 17: Material balance of step 1 of process A.....	40
Figure 18: Material balance of step 1 of process B.....	40
Figure 19: Material balance complete process A.....	41
Figure 20: Material balance of complete process B.....	42



## List of tables

Table 1: Activity concentration from one IAEA standard reference material. ....	23
Table 2: Composition of the PGL sample (code: 20-1452) measured by ICP-OES, ion chromatography and alpha spectrometry in comparison with the background value (Seawater, SW).....	26
Table 3: Radiological characterization of PGL and liquid fraction measured by alpha-spectrometry.....	32
Table 4: Solid and reactive mass.....	32
Table 5: Waste/Typical Soil relation for metals.....	37
Table 6: Radiological characterization of solid fraction measured by alpha-spectrometry.....	38
Table 7: Final effluent obtained and its comparison with limit values (Decreto 109/2015). ....	43
Table 8: Concentration (mg/kg) and transfer factor (%) (in parentheses) obtained after leaching test of samples and its comparison with Decreto 646/2020 (Landfill disposal Regulations). ....	45
Table 9: Natural radionuclides activity of samples obtained after leaching test. ...	46
Table 10: Comparison of the chemical composition of phosphate rocks from different deposits around the world. Jarvis et al. (1994); Damasceno (1989); Mc. Clellan (1989); Born (1989). ....	51

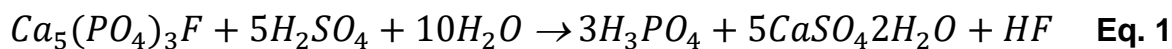


## 1. INTRODUCTION

Phosphogypsum (PG) is the main waste generated during the wet process manufacture of phosphoric acid, wherein rock phosphate and sulfuric acid are used as raw materials. The interest of phosphoric acid is mainly because of production of fertilizers, which have a high world demand, based on global crop production in the agriculture field. The global supply of phosphoric acid would increase by 1.5% per year between 2018 and 2023, while demand would grow at 1.4% p.a. (FAO- IFA, 2019).

The phosphoric acid production is based on the dissolution of the raw material, called “Phosphate Rock” (PR), by adding sulphuric acid (70 %), generating phosphoric acid (PA) and a white solid named phosphogypsum (PG), which more than 95% is calcium sulfate dihydrate ( $\text{CaSO}_4 \cdot 2\text{H}_2\text{O}$ ) (Bolívar et al., 1996; 1998). Large quantities of PG are generated from the conversion of phosphate ore into phosphoric acid by sulfuric acid attack. In 2022, the potential supply of phosphoric acid fertilizers is expected to reach about 63.7 million tons (FAO, ORG, 2019). The world annual generation of PG was estimated in 300 Mt, which implies to consume about 240 Mt of PR (USGS, 2017; Heffer and Prudhomme, 2016). The most common management of PG is its storage in large stacks which reach more than 50 m height (IFA-2011).

There are some chemical differences in the compounds obtained as products, depending on the origin of the mineral used in the production process. There are ores such as fluorapatite ( $\text{Ca}_{10}(\text{PO}_4)_6\text{F}_2$ ), hydroxyapatite ( $\text{Ca}_{10}(\text{PO}_4)_6(\text{OH})_2$ ), carbonate-hydroxyapatite ( $\text{Ca}_{10}(\text{PO}_4, \text{CO}_3)_6(\text{OH})_2$ ) and francolite ( $\text{Ca}_5(\text{PO}_4, \text{CO}_3)_3\text{F,OH}$ ), which have in common the apatite group of calcium phosphate as the main ore from which the acid is obtained. Specifically, in Huelva, the used ores were mainly fluorapatite and the complete process respond to the following equation:



As it can be seen in the equation, hydrogen fluoride gas is also generated as a non-main product and this is collected and sent into scrubbers to be absorbed in water, so a hydrofluoric acid weak effluent is produced. This effluent flow is mixed with the PG and it is also deposited into the stockpiles. Moreover, when the solid is separated from the acid by filtration, it need to be washed several times to regain the remaining phosphoric acid contained in the PG. After this washing, the PG is sent to the piles for its storage.



In Huelva, there was two periods of management of the industrial process. The first period was from the beginning of the industry, in the year 1968, to 1997. In this time, 20% of phosphogypsum leachate was directly pumped with seawater into the Odiel Estuary, and the remaining 80% was released into suspension in the stacks, then PG was decanted with the used water ( $\text{pH} \approx 2$ ) and a high concentration of contaminants ending up into the Tinto estuary without any treatment.

In the year 1998, another period started, and the management was identified by a closed system, in which PG pumped is done with freshwater into the stacks and then, after decantation of PG, the used water is re-sent to the industry plants. This new PG management system significantly reduced the pollutants emissions more than 95%. The production of PA, and in consequence, of PG, ended 31<sup>st</sup> December 2010 because of resolution of Supreme Court of Spain.

During this period in which the fertilizer industry was being operated, PG was deposited in a land near the Industry Complex in Huelva. It was estimated that about 80-100 Mt of PG were stored in piles that reach up to 20 m height in zone 2, and about 5 m in the rest of the zones (**Figure 1**).

There are differences between the zones. The zone 1, which represents about 30% of the total disposal area is now restored and revegetated. These tasks were done between the years 1990 and 1992, and the constructive restoration package was form by 40 cm soil layer. On the other hand, several years later, among years 1997 and 2009, the zone 4 was restored because of disposal of Huelva and Andalusia governments. The zone 4 represents near 20% of the total area and in this case, the restoration was done with a superior covering package composed by a 1 m building waste layer, a 2 m inert industrial waste layer and a 30-50 cm layer of topsoil.

However, nowadays there are zones 2 and 3 which represents near 50% of the disposal area and are openly exposed to environmental weathering, which contributes to the formation of leachates in raining periods. The piles have a series of perimeter channels for collecting leachates from PG weathering, but there are numerous points and diffuse sources of edge outflows that discharge into the estuary (Pérez-López et al., 2016a) (Papaslioti et al., 2018).



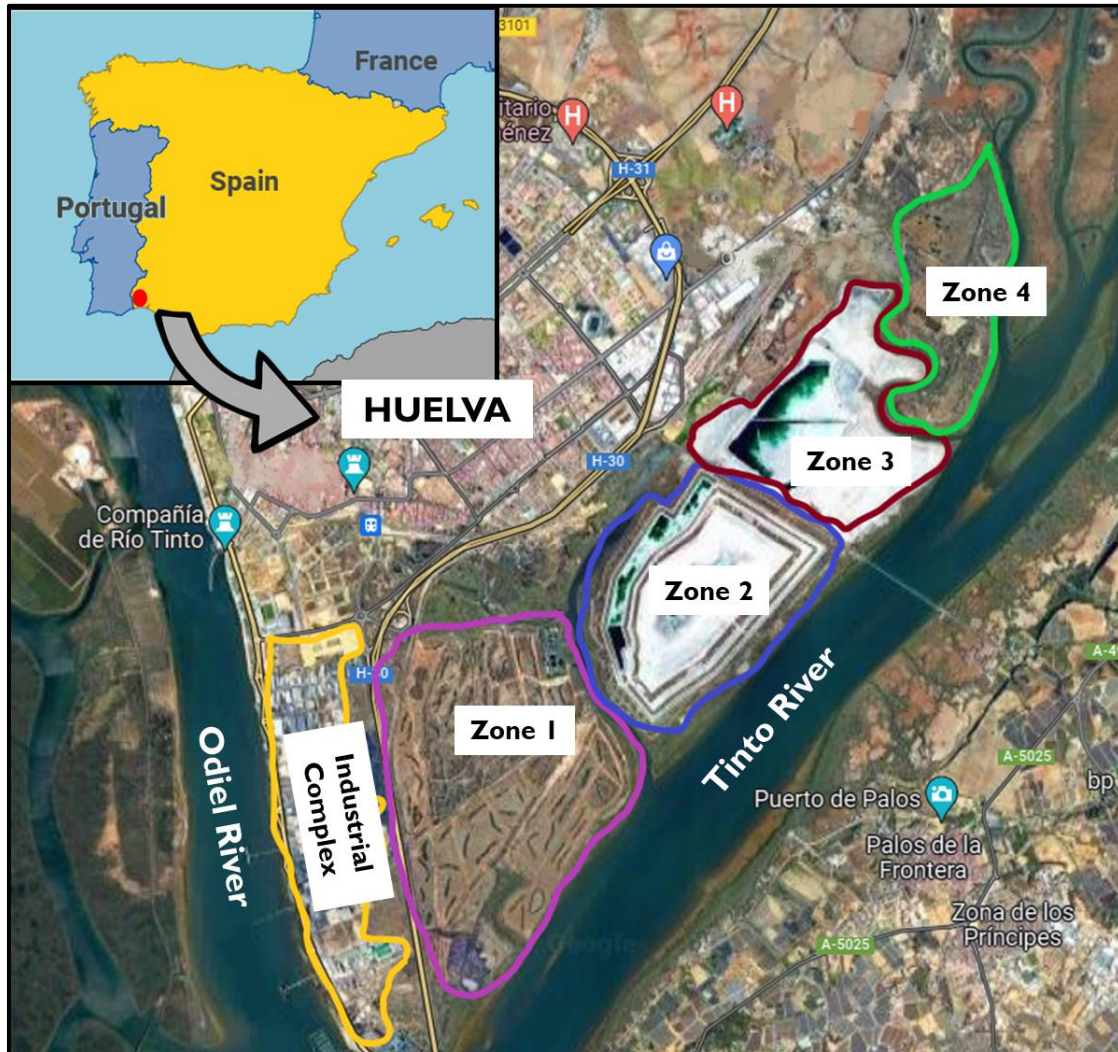


Figure 1: Location of the city, Industrial Complex and the PG stacks.

The company who is responsible for the piles has been proposed in September 2014 a remediation project to zones 2 and 3, which are still without any kind of protection. The project was approved by the National Court in October 2020 and consists of covering the PG surface with a geomembrane, followed by a layer of 60 cm compacted clay, a drainage layer of coarse material and a revegetated soil layer of about 1 m height at the top.

The most important condition imposed by the competent authorities to the remediation project is that all the produced leachates during the next 30 years after restoration need to be cleaned before their release into the estuary waters, according to the Decree 109/2015 for the heavy metals discharge limits.



## 1.1 Environmental problem

The phosphate industry is classified as a NORM (Naturally Occurring Radioactive Material) activity, since the raw material often contains natural radionuclides activity concentrations higher than the established thresholds by the EU Directives (EU Directives, 2013) and the Spanish regulation (CSN, 2011), and consequently this radiological and environmental problem has an international dimension.

The phosphate rock used in Huelva until 2010 contained concentrations of  $^{238}\text{U}$  and daughters around  $1.5 \cdot 10^3$  Bq/kg, which is about 50 times higher than the natural soils ones, while the  $^{232}\text{Th}$  series radionuclides and  $^{40}\text{K}$  levels were below the natural background, around 10 Bq/kg and 30 Bq/kg, respectively (Bolívar et al., 2009). The majority of uranium present in the raw material (more than 85% of U) remains in dissolution associated to the phosphoric acid, while more than 95% of the reactive elements ( $^{226}\text{Ra}$ ,  $^{210}\text{Pb}$  and  $^{210}\text{Po}$ ), and 70% of  $^{230}\text{Th}$ , remain in the PG (Bolívar et al., 1998, 2009).

Previous studies have characterized the leachate of the PG piles by the measurement of natural radionuclides, heavy metals, and other species as phosphates and fluorides. It was also demonstrated that only lateral leaching flows are produced, being negligible the liquid outflows by the base of the stacks (Guerrero et al., 2019). These lateral leaching flows have been estimated around  $3 \cdot 10^5$  m<sup>3</sup>/y (Pérez-López et al., 2016; TRAGSATEC, 2012), which implies an annual significant contribution of radionuclides and heavy metals from the PG pile into the Tinto River Estuary (about  $1 \cdot 10^{11}$  Bq of  $^{238}\text{U}$ ,  $1 \cdot 10^{10}$  Bq of  $^{210}\text{Po}$  and  $7 \cdot 10^8$  Bq of  $^{230}\text{Th}$ ).

In conclusion of these points, the Nuclear Safety Council (CSN) recognizes the PG stacks as a radiological contaminated area, principally due to the presence of U-series radionuclides ( $^{230}\text{Th}$ ,  $^{226}\text{Ra}$ ,  $^{210}\text{Pb}$ ,  $^{210}\text{Po}$ ) in a range of 500-1000 Bq/kg.

The central problem managed in this work is the environment emission of radionuclides and heavy metals from the unrestored PG piles (zones 2 and 3), which can be released by lateral outflows until reaches the estuary (**Figure 2**). There are previous studies about characterization of the leachates from the PG stacks taken in the perimeter channel, which evidences that these waters have a high acidity (pH < 2), and high concentrations of total phosphorus (10000 mg/L), fluorides (5000 mg/L), sulfates (4200 mg/L), U isotopes (25 mg/L), and metals such as K (250 mg/L), Mg (600 mg/L), Ca (1600 mg/L), Na (3500 mg/L), Cl (2000 mg/L) and Br (100 mg/L) (Perez-Lopez et al, 2016; TRAGSATEC, 2011).



**Figure 2:** Leachate from the perimeter channel.

The concentrations in the acidic waters of the piles (pore water, surface water or outflows water collected in the perimeter channel) are variable according to the solubility of the different elements and the time of the year when the samples are collected.

In addition, the estuary of Río Tinto is affected by acid mine drainage from the pyritic belt of Huelva, and it means a high contribution of heavy metals concentration such as Zn (45 mg/L), As (20 mg/L), Al (20 mg/L), Fe (70 mg/L), Mn (12 mg/L), Cu (8 mg/L) and radionuclides ( $^{238,234}\text{U}$ ,  $^{232,230,228}\text{Th}$ ,  $^{226,228}\text{Ra}$ ,  $^{210}\text{Pb}$ ,  $^{210}\text{Po}$ ). Because of this, it is a concern that the contribution of pollutants from PG leachate in the estuary is not negligible. Moreover, there are previous studies in the same area that confirm the significantly contribution of radioactive contamination along the Tinto estuary. (Bolívar et al., 2002) (Periáñez et al., 2013).

The PG leachates (PGL) are a worldwide environmental concern, so that its prevention and treatment options are a case of frequent study. It is estimated that between 3000 Mt of PG is stocked in at least 50 countries all over the world and every year PG is generated in a ratio of 175 Mt/y (International Phosphogypsum Working Group, PGWG).

Worldwide, China is the largest producer of phosphoric acid for the fertilizer industry and therefore of phosphogypsum. From 2001 to 2009, the production of phosphoric acid in China underwent a large increase from 7.4 Mt to 13.7 Mt, which represents 41.7% of world production in 2009. During the years 2010, 2011 and 2012, the fertilizer industry continued to increase being the volume of phosphoric acid production of 17.9 Mt, 14.6 Mt and 19.9, respectively. (PGWG, 2014).

India is another major producer of phosphogypsum. It is estimated that from 2006 to 2012 they have generated 9.4 Mt of phosphoric acid and about 43 Mt of phosphogypsum. In the United States, since the mid-1980s, phosphogypsum production has been around 40 to 47 Mt per year. The central Florida region is one of the largest producers, generating an estimated 32 Mt of phosphogypsum per year and having about 1000 Mt in storage. (US-EPA, 2012).





## 1.2 Process and treatments of acid leachates

There are two types of treatment methods for acid effluents: passive and active treatments. While in passive treatment the effluent is passed through a solid medium whereby geochemical and biological processes improve the quality of the water, requiring generally relatively little resource input of energy and materials once in operation, in active treatments, the water is treated in a controlled process, where often is required continuous input of resources to sustain the process.

Passive systems present the advantage of being self-sustaining with sporadic maintenance, and very low operating and capital costs, but the quality of the final effluent is often poorer. Moreover, this kind of treatment approaches are economically attractive but have some limitations. They are best suited to the treatment of waters with low acidity ( $\text{pH} > 2$ ), low flow rates ( $< 50 \text{ L/s}$ ), low acidity loads ( $< 150 \text{ kg of CaCO}_3$ ), and the maximum pH attainable is limited ( $< 8$ ), where the key chemical outcome is near to a neutral pH and associated low metal concentrations (Taylor et al., 2005; Humphries et al., 2017).

In the active treatments, the range of application is adapted to all flow rates, especially high flow rates. Although operating and capital costs can be higher than in passive methods, the quality of effluent obtained is better and it has some potential for cost recovering by selling of the product water and metals obtained, so this can be considered as a great advantage over passive treatments (Nleya et al., 2016). Conversely, the active treatment requires use of chemicals, operative and maintenance staff, and electrical and mechanical sources to perform efficiently. Depending on the composition of the liquid to be cleaned and of the quality required to the final obtained water, the active treatment could include, chemical treatment (precipitation steps), biological treatment, membrane technologies or ion exchange.

Neutralization is the most common process used for acid effluents treatment, since increasing the pH up to alkaline conditions produces precipitation of most metals. The most common neutralizing materials used to introduce alkalinity and clean acid effluents are: calcite ( $\text{CaCO}_3$ ), hydrated lime ( $\text{Ca(OH)}_2$ ), quicklime ( $\text{CaO}$ ), dolomite ( $\text{CaMg(CO}_3)_2$ ), magnesite ( $\text{MgCO}_3$ ), caustic magnesite ( $\text{MgO}$ ), alkaline waste as fly ash, sodium carbonate, sodium hydroxide, or ammonia (Taylor et al., 2005; Nleya et al., 2016).

Traditionally the main treatment for pollutants removing from acid effluents is the increase of pH by using alkaline chemical reagents (Jones and Cetin, 2017), such as  $\text{CaCO}_3$ ,  $\text{Ca(OH)}_2$ ,  $\text{Na(OH)}$ ,  $\text{Mg(OH)}_2$ , etc. However, these reagents are expensive, and their use may involve the generation of large quantities of sludge



without any added economic value due mainly to the difficulty of recycling their constituents, resulting in high management costs (Kefeni et al., 2017).

### **1.3 Circular economy**

Similar to other sustainable development models, circular economy addresses sources and production efficiency, slower material flows rather than linear economic models, and lower resources extraction without reducing economic activity (Velenturf and Purnel, 2021). Besides, circular economy is stated as a continuous positive development cycle that conserves and enriches natural capital, optimizes resource yields, and reduces system risks by managing finite stocks and renewable flows. (EU, 2017).

The Law 7/2022, of April 8, on waste and contaminated soil for a circular economy in Spain incorporates the principle of hierarchy in the production and management of waste to focus on prevention, preparation for reuse, recycling or other forms of recovery, including energy recovery, taking into account the European guidelines to transform countries into a "recycling society" and in this way, to contribute to the fight against climate change. This law transposes the European Directive 2008/98/CE about waste management and incorporates two concepts: by-products and the end to waste condition. A by-product is considered to be the residue of an industrial process, which by direct application serves as raw material in a different process. The end of waste condition is related with specific criteria that certain types of waste must comply so that they can cease to be considered as residue. This mean they need a valorization process in order to be applied as a by-product in another industrial process.

On this base, the phosphogypsum piles remediation project that have been approved aims to use techniques of sealing, drainage and coating as the best option considered for minimizing the environmental impact of the PG stacks. Moreover, it is important to consider that the generated wastes in the treatment could be valorized or reused, to impulse the circular economy.

The investigation group has already worked in neutralization of phosphogypsum leachate with different alkaline reagents such as  $\text{CaCO}_3$ ,  $\text{Ca(OH)}_2$ ,  $\text{NaOH}$ ,  $\text{Mg(OH)}_2$  or  $\text{Na}_2\text{CO}_3$ , and they have already demonstrated that they are effective for the removal of contaminants since they reduce their concentration with the increasing of pH. The main conclusions are that contaminants achieve the regulations limits for the discharge into coastal waters when neutralizers with Ca are used.



The aim of this work is to test sequential neutralization process at steps related with expected wastes, so that the wastes obtained can be easily valuable or reusable, in concordance with the philosophy of circular economy.

## 1.4 Objectives

### 1.4.1 General objective

Following the line of investigation in the research group "Radiation Physics and Environment" from the University of Huelva (UHU), and focusing on the environmental problem related with the phosphogypsum piles located near the city of Huelva, the principal objective of this work is to: conduce physicochemical, mineralogical and radiological characterization of the wastes generated during optimized process for the neutralization of PG leachates, and identify the potential ways for its valorization, considering the available technologies and their economic viability, all within the circular economy point of view.

### 1.4.2 Specific objectives

To achieve the previous central objective, the following specific objective were established:

1. Carry out the optimized sequential neutralization process for phosphogypsum leachates, which has been previously developed by another member of the research group.
2. Carry out a physicochemical and radiological characterization of the solid and liquid fraction of wastes obtained in each of the stages of the sequential neutralization process of the phosphogypsum leachate.
3. Analyze the potential environmental impact of the final products/wastes obtained and their environmental implications.
4. Carry out a bibliographical compilation about the alternatives and technologies available for the valorization of the obtained wastes.
5. Carry out a diagnosis of the valorization alternatives for the wastes generated in each stage of the neutralization process.

## 2 MATERIALS AND METHODS

### 2.1 Sampling

A leachate sample was taken in the perimeter channel from zone 2 of the PG stacks, which collects all the leachate produced above its level (**Figure 3**). The sample was collected in September 2020, and approximately 20 L were taken. The physicochemical parameters (pH, electrical conductivity and redox potential) were



measured in situ by using portable equipment. Later in the laboratory, the sample was coded (20-1452) and filtered through a vacuum system, using cellulose nitrate filters of 0.45  $\mu\text{m}$  pore size.

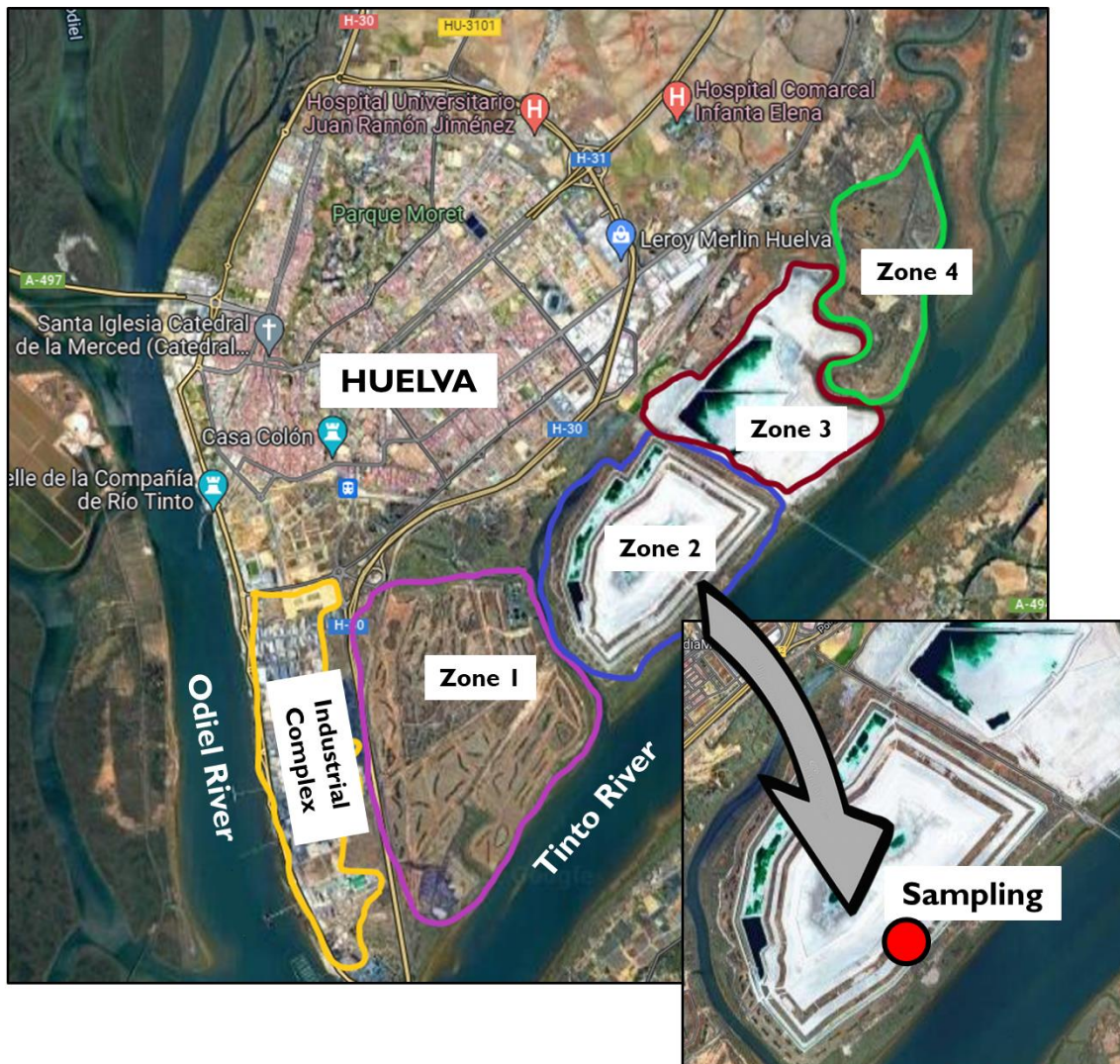


Figure 3: Location of sampling area.

## 2.1 Design of experiments

By analyzing the composition of the phosphogypsum leachates, considering that the highest concentrations correspond to phosphorus (at  $\text{pH} = 2$  is mostly as  $\text{H}_3\text{PO}_4$ ) and fluor (in the PGL more than 90% of  $\text{HF}$  is not dissociated), followed by the  $\text{Ca}^{2+}$  and  $\text{SO}_4^{2-}$ , it is expectable that the best cleaning processes should be based on increase the  $\text{pH}$  by using neutralizing agents containing  $\text{Ca}$  such as  $\text{Ca}(\text{OH})_2$ ,  $\text{CaCO}_3$ , or  $\text{CaO}$ , since taking into account the solubility constants of their salts, will firstly precipitate calcium fluorides, followed of calcium phosphates and metals hydroxides which could co-precipitate other metals and natural radionuclides.





According to the results obtained in previous studies, the fluorides will be precipitated for about pH = 3-4, while calcium phosphates precipitate at pH = 5-7 and all metals as Fe, Al, Cr, Cd, U and Zn will be 100% removed for pH > 11-12.

The pH of the stages was selected based on the precipitation solids that were obtained in a previous investigation work, so in this case, an optimized sequential neutralization process in two steps was conducted. The first phase of the process consists of reaching a pH of 3.5 and the second phase is up to pH 12. The reason to do these specific stages is because the previous studies have been demonstrated that at pH around 3-4, the fluorides contained in the PGL precipitate with added  $\text{Ca}^{+2}$  forming up calcium fluoride, which has a special interest on its valorization and, on the other hand, the second step is conducted in order to precipitate the phosphates forming a second waste in view of its valorization or reused.

For some elements as As, it is necessary to reach up pH = 12, to have an effective percentage of precipitation, although most of elements (Fe, Al, Cr, Cd, U and Zn) precipitate at pH = 5-6, the main idea was to optimize the process in two steps, so that the second phase is ending at pH = 12.

The design of experiments is based on two processes conducted in parallel: the process A is made using calcite ( $\text{CaCO}_3$ ) in the first phase and then hydrated lime ( $\text{Ca(OH)}_2$ ) in the second step, while the process B is conducted with hydrated lime in both phases, as can be seen in **Figure 4** and **Figure 5**. These reagents were selected to evaluate the different solids that are formed in each case.

In both processes, 2 L of phosphogypsum leachate were used and the experiments were made by duplicate, consisting of adding the specific alkaline reactive whose mass was previously determined considering the pH that need to be reach.

In step 1 of process A, 25 g theoretical of  $\text{CaCO}_3$  were estimated, while in step 1 of process B, 15 g theoretical of  $\text{Ca(OH)}_2$  were supposed. In step 2 of both processes were estimated 54 g theoretical of hydrated lime to achieve the pH proposed, considering the titration curves.

Basically, the experiment consists of adding the alkaline agent in quantities of approximately 2-5 g, depending on the total mass estimated, and stirring the solution with a magnetic stirrer system. The pH is measured in intervals of 5-10 minutes, when it is stable and the desirable pH is reached. Once this occur, the solution is filtered using cellulose nitrate filter of 0.8  $\mu\text{m}$  pore size, obtaining, on one hand, the liquid fraction and on the other hand, the solid fraction, which is dried in oven at 50 °C until constant mass. Then the solids are weighed and reserved for posterior



analysis and the parameters such as pH, conductivity and redox potential are measured in the liquid fraction.

The samples obtained were codified considering the process (A or B), the step of the process (1 or 2), and the fraction (liquid or solid), so that, the sample LA1 correspond to Liquid fraction of phase 1 from Process A. In brief, 4 sampling batches for each process were obtained, 2 for each step (liquid and solid).

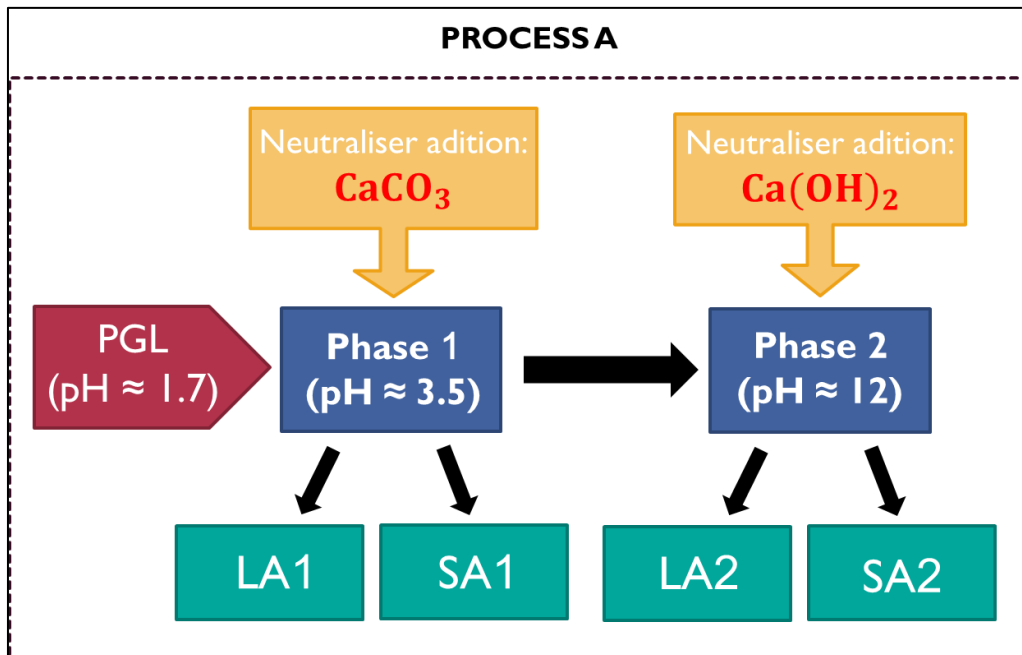


Figure 4: Diagram of sequential neutralization process A

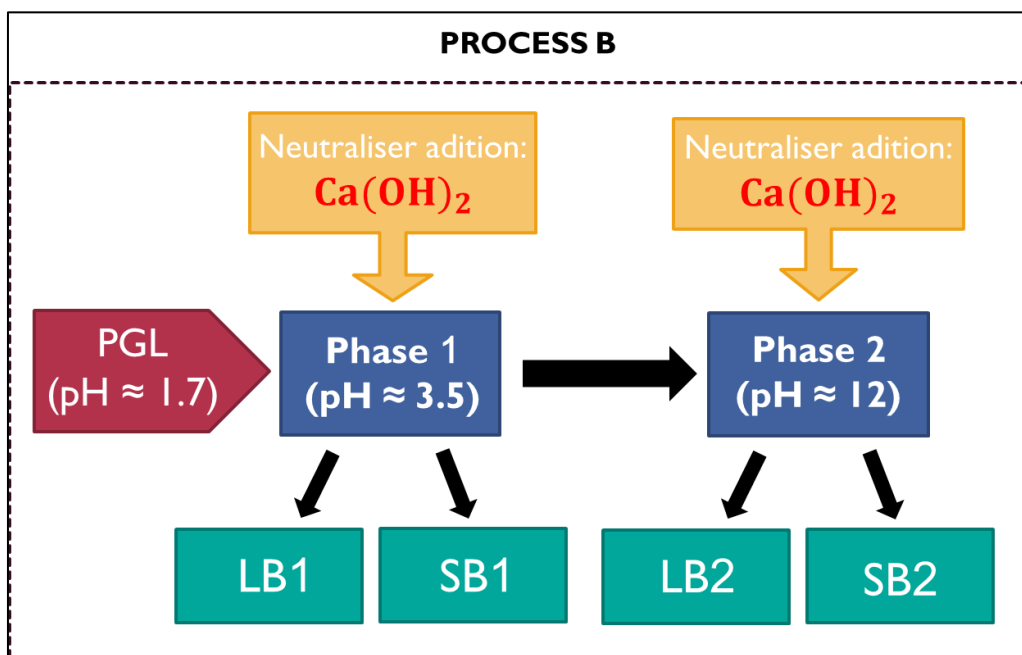


Figure 5: Diagram of sequential neutralization process B



## 2.2 Characterization techniques

### 2.3.1 Physicochemical techniques

#### 2.3.1.1 Inductively coupled plasma mass spectrometry (ICP-MS)

The technique of inductively coupled plasma mass spectrometry (ICP-MS) is a variation of analytics techniques based on mass spectrometry. This technique consists of sample ionization and ion separation in relation with the charge/mass ratio ( $z/m$ ), to get its posterior counting. The area from each peak is proportional to the concentration of an element in the sample.

The sample need to be introduced in the device as a liquid. It is absorbed through a capillary by peristaltic pumps, in order to introduce the sample in the nebulizer where it is converted to small drops to homogenize the supply of sample to the plasma. In the plasma it is produced the ionization of the sample, where the drops diameter does not exceed 10  $\mu\text{m}$ .

Then, the ions from the ICP source are collimated and focused into the entrance aperture of the mass spectrometer by the electrostatic lenses. The function of the quadrupole mass spectrometer is to separate the ions based on their charge/mass ratio, to then pass to the detector.

Once the sample reaches the detector, the measured data is quantified. This quantification is achieved by comparing the counts measured in an unknown sample with those of a substance with a known amount of the element of interest.

This technique is suitable especially for isotope ratio and trace analysis of elements, whose instrumental detection limits (IDL) is in the range from 1 ppt to 10 ppb, depending on the element.

The ICP-MS technique was conducted at the Accredited Laboratory of Canada (ACTLABS, Ontario) and the spectrometer Perkin Elmer Sciex ELAN 9000 was used. With the purpose to generate a quality control of the equipment accuracy, a blank reagent and a standard reference material with the replication of samples were done and, in all cases the analytical data accuracy varies from  $\pm 5\text{-}10\%$ .

#### 2.3.1.2 Inductively coupled plasma optical emission spectrometry (ICP-OES)

The technique of Inductively Coupled Plasma Optical Emission Spectrometry (ICP-OES) is based on the vaporization, dissociation, ionization and excitation of the different chemical elements of a sample inside a plasma, in a similar way to that seen in the previous section. While in the ICP-MS the charge/mass ratio of the ions is measured, the ICP-OES technique measures the radiation emitted by the different atoms, through an optical detector.



As in the ICP-MS case, the sample need to be introduced as a liquid, then it is absorbed through a capillary by peristaltic pumps and introduced in the nebulizer where it is converted in aerosol.

The plasma is obtained inside the torch because of a high frequency current generated by an oscillating magnetic field, where reaches the argon that sustains the plasma. The sample is nebulized in small drops, and it ascends in the torch to proceed to the drying and evaporation. Finally, each atom loses one or more electrons when entering the zone of maximum temperature of the plasma. Leaving this zone, the electrons return to their state and during this de-excitation process, electromagnetic radiation emissions are produced in the UV-visible zone. These radiations, characteristic of each moment, are separated according to their wavelength and finally their intensity is measured.

For this, an optical system is available, responsible for analyzing the spectrum emitted by the plasma, in addition to a signal processing system, which makes possible a qualitative and quantitative analysis from the radiation emitted.

The quantification system consists on measuring the intensities of different patterns and compare them with known concentrations for each element to be analyzed.

In the case of ICP-OES, it is suitable for trace elements that are presented in high concentrations in the sample (100 to 1000 ppm). This technique also was conducted at the Accredited Laboratory of Canada (ACTLABS, Ontario) and the equipment used was an ICP-OES Agilent Axial 730-ES. In addition, to verify the accuracy data, a blank sample and a standard reference material were measured. The samples also were done by duplicate and the variation goes between  $\pm 5-10\%$ .

#### *2.3.1.3 Ion Chromatography*

Ion chromatography is one of the most important methods for the analysis of trace anions, enhancing the separation of molecules as a function of their electric charge.

The sample is pumped through two different ion exchange columns in succession, then through a conductivity suppressor device and finally a conductivity detector.

The two anion exchange columns, a pre-column and the separation column itself, contain an anion exchange resin inside. The ions presented are separated into discrete bands based on their affinity for the exchange sites on the resin.

The conductivity suppressor is a device made up of a cation exchange resin that reduces the baseline conductivity to a very low value and simultaneously converts the anions presented in the sample into the respective acids that have higher





conductivity. The separated anions in their acid form are measured using an electrical conductivity cell.

The identification of the anions is carried out by comparing the retention times of the peaks of each analyte, and the quantification by measuring the area of those peaks with respect to a calibration curve generated from standard solutions of known concentration.

This technique was conducted in Central Research Services at the University of Huelva. The equipment used was the ion chromatographer DIONEX DX-120, which is a complete system with an isocratic bomb, a conductivity detector, an automatic sampler AS40 and an incorporated software called PeakNet. In order to check the accuracy analytical data, the comparison with reference standard solution for certain anions is done and, in addition, there are made a blank and duplicated measurements.

#### 2.3.1.4 X-Ray fluorescence (XRF)

X-ray fluorescence (XRF) is a spectroscopic technique that uses the secondary or fluorescent emission of X-radiation generated by exciting a sample with an X-radiation source. The incident or primary X-radiation ejects electrons from inner shells of the atom. The electrons from the outermost shells occupy the vacant places, and the excess energy resulting from this transition is dissipated in the form of photons, fluorescent or secondary X-radiation, with a characteristic wavelength that depends on the energy gradient between the electron orbitals involved, and an intensity directly related to the concentration of the element in the sample.

The equipment has a detector which measures the intensity of the X-rays emitted by the sample. Then, it has a multichannel analyzer that designates an energy value to each height pulse, creating a XRF spectrum. The net area of the peaks is proportional with the presence of the element in the sample, so that the exact value of the proportionality is derived by comparison with a known material such as mineral or rock standards.

Major elements were determined by X-ray spectrometer wavelength dispersion (model ZETIUM) in the Central Research Services of the University of Seville (Spain). The OMNIAM semi-quantitative method is a general wavelength dispersive measurement method (WDXRF). At the SGI X-Ray Laboratory, the following criteria has been taken to determine the relative uncertainties for each element present in the sample according to its concentration:

For elements presented between 15-100% the relative uncertainty will be 5%, for elements presented between 1-15% the relative uncertainty will be 10%, and for



elements presented between 0-1% the relative uncertainty will be 20%. After each adjustment of the OMNIAM semi-quantitative method, the measurement of some certified standards is carried out to verify that this criteria is met in most of the elements measured.

#### 2.3.1.5 X-Ray Diffraction (XRD)

X-Ray Diffraction methods are one of the essential tools for studying the crystalline structure of solids. One of the most common methods is the powder method, which allows the identification of crystalline phases and, applying the Rietveld refinement method, their quantitative analysis.

This procedure is based on the fact that each crystalline phase has its own characteristic diffractogram, depending on its internal structure and the types of atoms that compose it. On the other hand, X-ray diffraction only identifies crystalline phases and compounds from their diffraction spectrum, it is not a chemical analysis technique.

The disoriented powder method consists of irradiating with X-rays a sample made up of a multitude of crystals placed randomly in all possible directions. In this technique, the sample is milled into a fine powder (less than 10  $\mu\text{m}$ ) and placed into a sample holder. The geometry orientation used is Bragg-Brentano, where the X-rays emitted by the anode of the tube fall on the flat surface of the pulverized sample with an angle of incidence " $\theta$ " that varies as the sample rotates. At the same time, the detector mounted on a rotating arm rotates a double angle " $2\theta$ ", collecting a continuous background of radiation and a series of maximum that correspond to the X-rays diffracted by the reticular planes of the sample that are parallel to the surface. The equipment is connected to a computer equipped with the DIFRAC.-EVA software package and uses internal standards for the acquisition, treatment and evaluation of the data obtained, comparing the sample using the PDF-4 database (ICDD). The crystalline phases presented in a percentage less than 5% are not detectable, and in addition, it is added zincite (ZnO) as an internal standard for amorphous fraction determination.

The XRD was conducted at the Central Research Services of the University of Seville (Spain) and Bruker diffractometer model D8-Advanced A25 was used. For the quantification of the crystalline phases was used the "DIFRAC.TOPAS" software, according to the Rietveld method.



## 2.3.2 Radiometric techniques

### 2.3.2.1 Alpha spectrometry

The disintegration of certain radionuclides, fundamentally those with a high atomic number, in the different radioactive chains is produced by the emission of an alpha particle. Alpha spectrometry is called the technique that allows the qualitative and quantitative determination of radionuclides which emit alpha particles.

The measurements corresponding to the alpha spectrometry have been carried out with semiconductor detectors (Si), inside of an ion implantation vacuum chamber (EG&ORTEC). The detectors have a certified Full Width Half Maximum (FWHM) of less than 20 keV for a monoenergetic emission of  $^{241}\text{Am}$ , with a detection efficiency close to 25% for distances less than 10 mm. Its certified background is less than 30 counts per day corresponding to energies between 3-8 Mev. The detectors operate at a working voltage of 50 V and are connected to a conventional electronic chain, composed of a preamplifier, an amplifier, a digital analog converter and a multichannel analyzer.

Taking into account that alpha particles are absorbed in solid materials of few microns, in this technique it is necessary to minimize alpha particles self-absorption effects. In order to avoid the interferences, the radioelements need to be isolated and chemically purified to be electroplated on an acceptable material, applying a radiochemical process.

The investigation group has developed a radiochemical method for the alpha-particle spectrometry. This method consists on: preparation and sample collection, addition of tracers, sample dissolution, chemical separation, deposition onto counting discs, alpha spectrometer counting and calculation of tracer recovery and sample activity.

In case of the liquid fraction, the procedure starts with the addition of tracers because the samples are not previously treated. The solid samples were additionally digested in microwave following the EPA 3052 method, after the addition of tracers.

These tracers are used for evaluating the radiochemical process efficiency, since they are artificial radioactive isotopes with same chemical behavior than the radionuclide of interest, enhancing to calculate the efficiency with a radioelement of known activity.

In case of liquid and solid fraction, the tracers used were  $^{209}\text{Po}$  which a certified activity of  $77.9 \pm 1.9$  mBq/mL and  $^{232}\text{U}$  which a certified activity of  $138.9 \pm 0.6$  mBq/mL. Once the tracers are added and the sample digested, in case of solids,



they are evaporated to dryness and leaved with 10 mL of 8 molar of nitric acid, to conduct the next step which is the extraction of elements with tributyl-phosphate (TBP).

In the funnels, it is added nitric acid where polonium remains and TBP where actinides elements tend to remain (U, Th, Pu, Am). Once the Po is isolated, the sample is evaporated to dryness and leaved with 10 mL of 2 molar of hydrochloric acid.

To the phase that remains into the funnel, it is added distilled water in order to extract the uranium. The next step is the deposition of Po and U. In case of Po, it is self-deposited in silver discs while U isotopes are electrodeposited onto stainless steel discs and carried to the spectrometer.

Lastly, the activity concentration of the radioelements is calculated with the counts from the alpha spectrometer. This radiochemical method developed at the laboratory of the investigation group is validated by participation in intercomparison between different national or international labs and, in addition, blanks and replicates are done in order to make a quality control of the results obtained. Also, standard materials are measured. For example, in **Table 1** are shown the values of natural radionuclides from a certified referential material (IAEA 434). The z-score was calculated for uranium isotopes and they are under 2, meaning there are no serious differences between the measured and the certified values.

	Radionuclide	Measured value (Bq/kg)	Certified value (Bq/kg)	Z- score
IAEA 434 (SOIL)	$^{234}\text{U}$	$100 \pm 5$	$120 \pm 9$	1.91
	$^{238}\text{U}$	$108 \pm 5$	$120 \pm 11$	0.99

**Table 1:** Activity concentration from one IAEA standard reference material.

### 2.3.3 Leaching test

This test was conducted based on the norm UNE – EN – 12457-4 “Characterization of waste. Leaching. Compliance test for leaching of granular waste materials and sludges. Part 4: One stage batch test at a liquid to solid ratio of 10 L/kg for materials with particle size below 10 mm”. It is an adequate test to evaluate the mobility of both organic and inorganic compounds presented in liquids, solids and multiphase wastes.

The first step is to reduce the solid particles to a size less than 4 mm, when it is needed. Then, a quantity of  $2.5 \pm 0.1$  g of solid is weighted and mixed with a relation of extracting fluid of ten times. Generally, distilled water is used, but it is a function of the alkalinity of the solid phase. The sample is taken to a rotatory system and



rotated at  $30 \pm 2$  rpm for 24 hours. The temperature must be kept at  $22 \pm 3$  °C. After that, the sample is filtrated with a nitrocellulose filter of 4  $\mu\text{m}$  and parameters such as pH, electrical conductivity and redox potential are measured in the liquid with a multimeter equipment. The liquid is sent to posterior analysis such as ICP-MS/OES.

Once the Leaching Test was conducted, the concentration ( $C_i$ ) of a contaminant “x” (mg/kg) was calculated with the following equation:

$$C_i = C \left[ \frac{L}{M_D} + \frac{MC}{100} \right] \quad \text{Eq. 2}$$

Where  $C_i$  is the release of a constituent at L/S of 10 (in mg/kg dry mass); C is the content of a particular constituent in the eluate (in mg/L); L is the volume of the lixiviant used (in L); MC is the wet ratio content expressed as a percentage of dry mass;  $M_D$  is the dry mass of the test portion (in kg).

Additionally, the Transfer Factor was calculated as follow:

$$TF (\%) = \frac{C_i}{C_{i,s}} \times 100 \quad \text{Eq. 3}$$

Where:  $C_i$  is the concentration of the contaminant “i” in the Leaching Test at L/S of 10 (in mg/kg dry mass); and  $C_{i,s}$  is the concentration of the element “i” in the solid, both given in mg of the pollutant “i” per kg of waste (mg/kg waste).

### 3 RESULTS AND DISCUSSION

#### 3.1 Physicochemical characterization of phosphogypsum leachate (PGL)

The physicochemical and radiological characterization of PGL sample is shown in **Table 2**, as well as the composition of the background value corresponding to seawater (SW) (Guerrero et al., 2021; Papsalioti et al., 2020). As may be seen, the PGL presents a pH 1.7, which means it is a solution extremely acid compared with the seawater which has a neutral/alkaline pH (7.8). Moreover, the PGL has a lower electrical conductivity (30.2 mS/cm) and higher redox potential (656 mV) in relation with the background, which has EC of 61.0 mS/cm and Eh of 460 mV.

Regarding with element concentrations, as may be seen in the table, there are several elements that are in higher concentrations in the PGL, such as As, Cr, Cd, Pb and Cu which exceeds in 3 orders of magnitude the concentration in the SW, while Fe, Mn, U, Ni, Zn oversteps SW concentration in 2 orders of magnitude. There



are other elements as Al that also has a higher concentration of 1 order of magnitude superior in the PGL. On the other hand, some components like K, Mg and Na are in lower concentrations in the PGL than in the SW.

Concerning about the anion concentrations, as could be seen in **Table 2**, the phosphates are near 40 times higher than that contained in the seawater, along with fluorides that are 20 times higher in the PGL. In contrast, sulphates and bromides are in similar concentrations, while chlorides approximate 4 times higher in the SW than PGL. These concentrations are similar to those found in other studies performed in the same zone (Pérez-López et al., 2016b; Pérez-López et al., 2015).

The activity concentrations of natural radionuclides are also included in **Table 2**. The PGL sample mainly contains about 300 Bq/L of  $^{238-234}\text{U}$  and 40 Bq/L of  $^{210}\text{Po}$  where it is remarkable this high concentration, exceeding the background values four orders of magnitude. Because of the PGL composition exposed and its elevated pollutant load, it is evidenced the necessity to collect the leachate waters and treat them before they are discharged to the estuary.

Regarding with the phosphates concentration in the PGL, it is in the same order than previous characterization performed by the investigation group. So, the concentration of phosphates from sample 20-1124 collected in March 2019 is about 28500 mg/L of  $\text{PO}_4^-$ , and the sample 20-1452 used in this work has a phosphates concentration ( $\text{PO}_4^-$ ) of 31300 mg/L.



Parameters	PGL	Background value (Seawater, SW)	PGL/ SW
pH	1.7	7.8	0.20
EC (mS/cm)	30.2	61.0	0.50
Eh (mV)	656	460	1.40
<b>Element</b>	<b>C (mg/L)</b>	<b>C (mg/L)</b>	
Al	6.5	0.13	50
As	27.4	<0.002	$1.4 \cdot 10^4$
Ca	1660	440	3.80
Cd	7.8	<0.002	$3.9 \cdot 10^3$
Cr	22.1	<0.002	$1.1 \cdot 10^4$
Cu	8.7	0.004	$2.1 \cdot 10^3$
Fe	129	0.008	$1.6 \cdot 10^4$
K	268	440	0.60
Mg	906	1440	0.60
Mn	12.4	<0.002	$6.1 \cdot 10^3$
Na	4920	11700	0.40
Ni	5.6	<0.002	$2.8 \cdot 10^3$
Pb	0.8	0.003	$2.5 \cdot 10^2$
Zn	65.9	0.050	$1.3 \cdot 10^3$
U	20.5	0.003	$6.4 \cdot 10^3$
<b>Anion</b>	<b>C (mg/L)</b>	<b>C (mg/L)</b>	
F <sup>-</sup>	1960	111	18
Cl <sup>-</sup>	5250	21700	0.20
Br <sup>-</sup>	28	69	0.40
PO <sub>4</sub> <sup>-</sup>	31300	791	40
SO <sub>4</sub> <sup>-</sup>	4540	3288	1.40
<b>Radionuclides</b>	<b>Bq/L</b>	<b>Bq/L</b>	
Po-210	$39 \pm 0.2$	$0.0036 \pm 0.0004$	$1 \cdot 10^4$
U-238	$254 \pm 12$	$0.042 \pm 0.002$	$6 \cdot 10^3$
U-234	$248 \pm 12$	$0.041 \pm 0.002$	$6 \cdot 10^3$

**Table 2:** Composition of the PGL sample (code: 20-1452) measured by ICP-OES, ion chromatography and alpha spectrometry in comparison with the background value (Seawater,SW)

### 3.1 Samples characterization

The neutralization process of the PGL has been carried out with Ca(OH)<sub>2</sub> because it has been demonstrated in previous studies of the investigation group the contaminants are highly removed founding concentration of them lower than emission limit established for liquid effluents discharge and lower than seawater





background, in case of natural radionuclides. In addition,  $\text{CaCO}_3$  have been also selected with the purpose of compare both alkaline reagents, but only in the case of phase 1, because it has been noticed that  $\text{CaCO}_3$  only reaches a pH of approximately 6. This occurs because the solution acts as a buffer in that pH, meaning that it can absorb excess acids ( $\text{H}^+$ ) or base ( $\text{OH}^-$ ) without significantly change in its pH.

The physicochemical characterization as well as radiological of both fractions, liquid and solid, are shown in the following sections.

### 3.1.1 Liquid fraction

The composition of the liquid fraction obtained from the sequential neutralization process is shown in **Annexe 6.1**, as well as the physicochemical data of the original leachate used in the treatment process. In addition, the concentration of main and minor elements from both processes (A and B) are plotted in **Figures 6 to 9**.

Firstly, the parameters such as pH, electrical conductivity (EC) and redox potential (Eh) were determined for PGL and resultant liquid fractions. The pH that characterized the phases are 3.5 for step 1 and 12 for step 2. Also, the EC of both processes have similar values (24.3 mS/cm and 23.8 mS/cm for LA1 and LB1, respectively, and 19.1 mS/cm and 18.7 mS/cm for LA2 and LB2), producing a drop in the electrical conductivity in comparison with the original leachate, as it is expected because of the reduction in the dissolved salts.

Adding on, the redox potential passes from a positive value in step 1 for both processes (557 mV and 553 mV for LA1 and LB1, respectively) to a 163 mV and 177 mV for LA2 and LB2 in the second phase, indicating the reducing power of the final dissolution.

As may be seen, in process A, the concentration of elements such as Al (0.9 mg/L), Cr (3.6 mg/L), Fe (0.7 mg/L), Pb (<0.1 mg/L), and U (3.6 mg/L) have been reduced in the first step of the neutralization process (LA1). On the other hand, elements such as As (26.5 mg/L), Cd (7.3 mg/L), Mg (875 mg/L), Ni (5.4 mg/L), P (8900 mg/L), S (1440 mg/L), Si (463 mg/L), Si (38.8 mg/L) and Zn (45.6 mg/L) still remain in high concentration in the first step. These concentrations can be observed in the **Figure 6 and 7**.



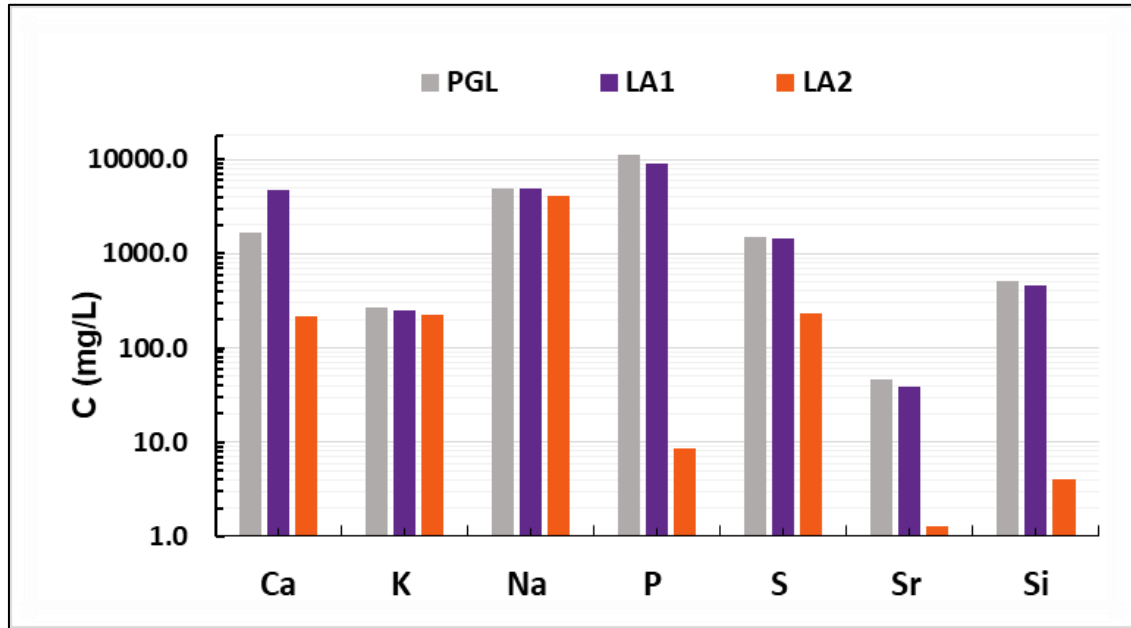


Figure 6: Concentration of main elements in liquid fraction in process A.

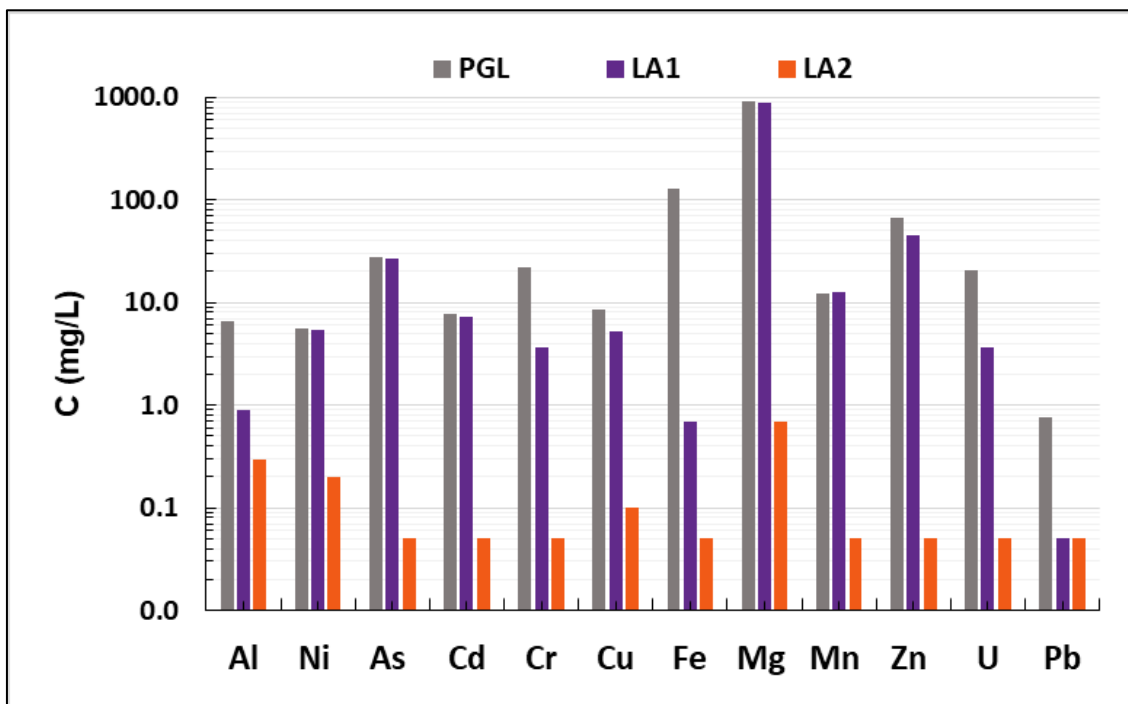


Figure 7: Concentration of minor elements in liquid fraction in process A.

In case of process B, where  $\text{Ca(OH)}_2$  is used in step 1, the results are similar, obtaining elements such as Al (0.9 mg/L), Fe (0.3 mg/L), Pb (<0.1 mg/L) and U (0.8 mg/L) that are completely precipitated in phase 1. Moreover, there are some elements that still remain in the solution in high concentration in step 1 of the process, such as As (26.1 mg/L), Cd (7 mg/L), Mg (886 mg/L), Ni (5.0 mg/L), P(8460



mg/L), S(1090 mg/L), Si(445 mg/L), Sr (36.8 mg/L) and Zn (38.6 mg/L). These concentrations are plotted in **Figure 8** and **9**.

For both processes, the concentration for the remaining elements of step 1 are significantly reduced in step 2 (LA2 and LB2), as it is in correspondence with the objective of the experiment. Some of the elements such as Al, Ni, As, Cd, Cr, Cu, Fe, Mg, Mn, Zn and U reach concentrations lower than the detection limit of the technique (LoD=0.1 mg/L), as it can be observed from **Figure 6 to 9**. Further, there are not slightly differences in concentration of elements comparing step 2 of process A with B.

The principal differences are presented in stage 1 of processes because a different reagent was used. It can be noticed that a higher concentration of certain elements is obtained in step 1 of process A with CaCO<sub>3</sub>, such as 1.3 times higher concentration of S, 1.8 times of Cr, 2.3 times higher concentration of Fe, 1.1 times of Zn and the most novel fact, 4.5 times higher concentration of U, comparing with process B. The concentration of the rest of elements are in the same order in step 1 of both processes.

Additionally, it can be observed that are elements such as K and Na that are in similar concentration in the original leachate and in the two steps of the treatment process, for process A and B. This means they are conservative elements that are not affected by the process.

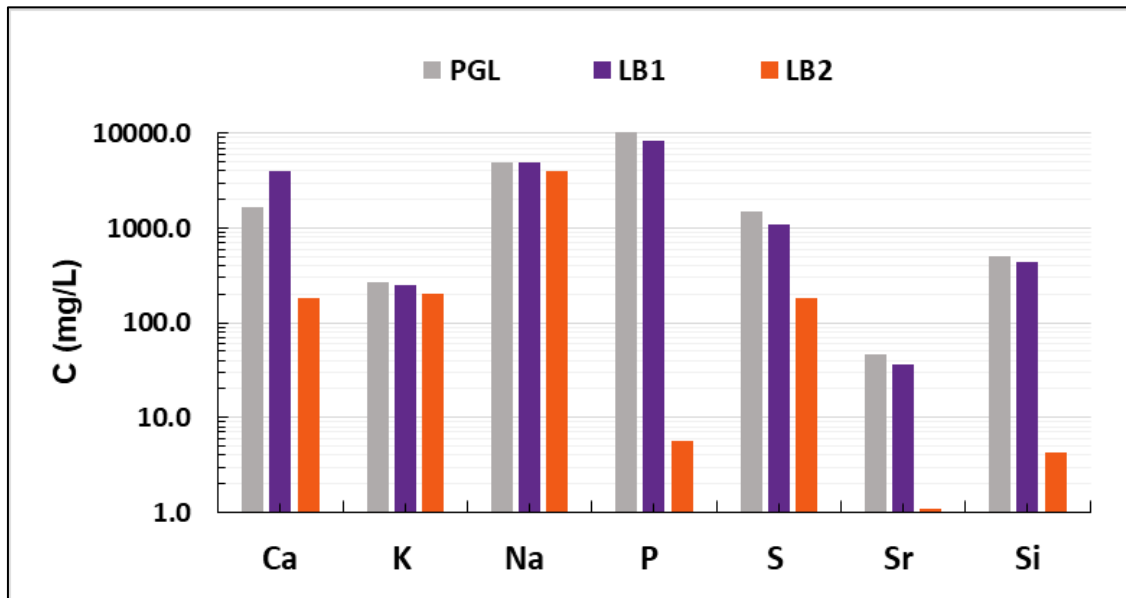


**Figure 8:** Concentration of main elements in liquid fraction in process B.

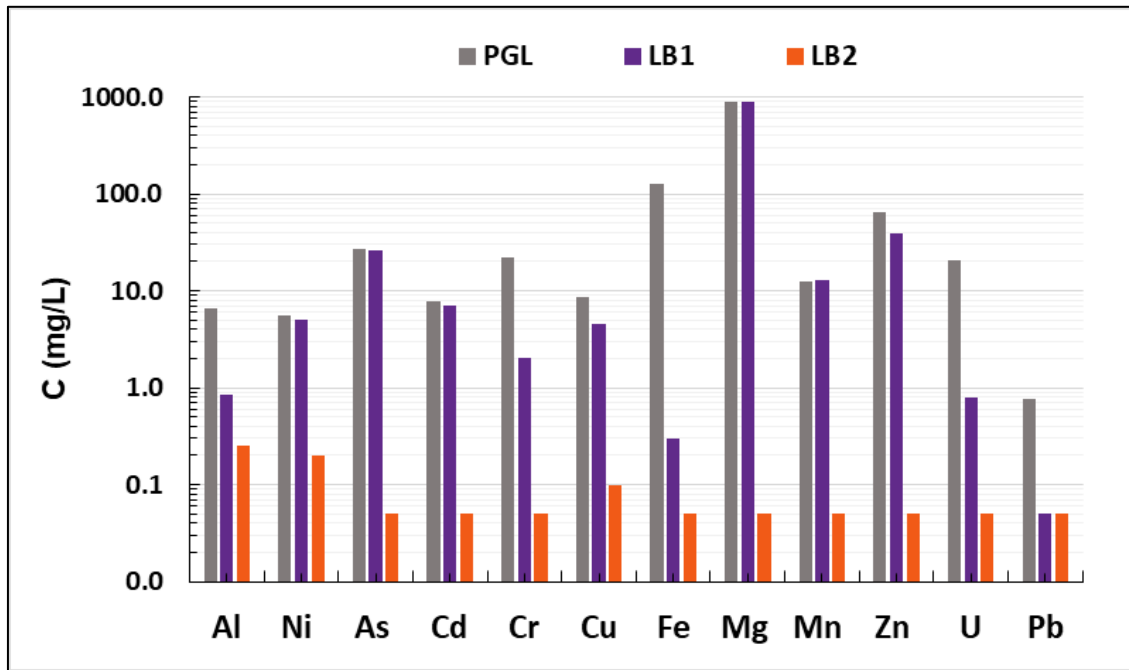


Figure 9: Concentration of minor elements in liquid fraction in process B.

In **Figure 10** there are presented the results from the ion chromatography test, and as it can be noted, there are practically no variation in the composition of nitrates, chlorides, and bromides obtained in the two processes, fact expectable by considering that these anions do not form insoluble sales with Ca. (Millán-Becerro et al., 2019)

In addition, it is worth highlighting that fluorides concentration in both processes decreases around 95% comparing their concentration in the original PGL and the final concentration observed in phase 1. Moreover, in phase 2 the fluorides are presented in the liquid fraction in a very low proportion of 0.9 mg/L and 0.7 mg/L (LA2 and LB2, respectively).

As it can be seen in the figure, the phosphates concentration does not decrease in appreciable quantities at pH = 3.5 (phase 1 of both processes) since it passes from 31300 mg/L in PGL to 27400 mg/L and 25900 mg/L in process LA1 and LB1, respectively, needing a higher pH to be reduced, as it can be noticed in phase 2 of both processes. It is important to point out that in step 2 of both processes precipitate the most of phosphates, since their concentration in the liquid fraction is 26.7 and 17.5 mg/L in LA2 and LB2, respectively.

The sulfates have a similar conduct than the phosphates, requiring a higher pH than 3.5 to decrease their concentration, to 645 mg/L and 488 mg/L in LA2 and LB2, respectively. In addition, it is observed that, when  $\text{Ca}(\text{OH})_2$  is used, comparing with the use of  $\text{CaCO}_3$ , the concentration of phosphates and sulfates in the liquid fraction



in step 2 is around 1.3-1.5 times lower, which is an important different between both processes related with liquid discharge.

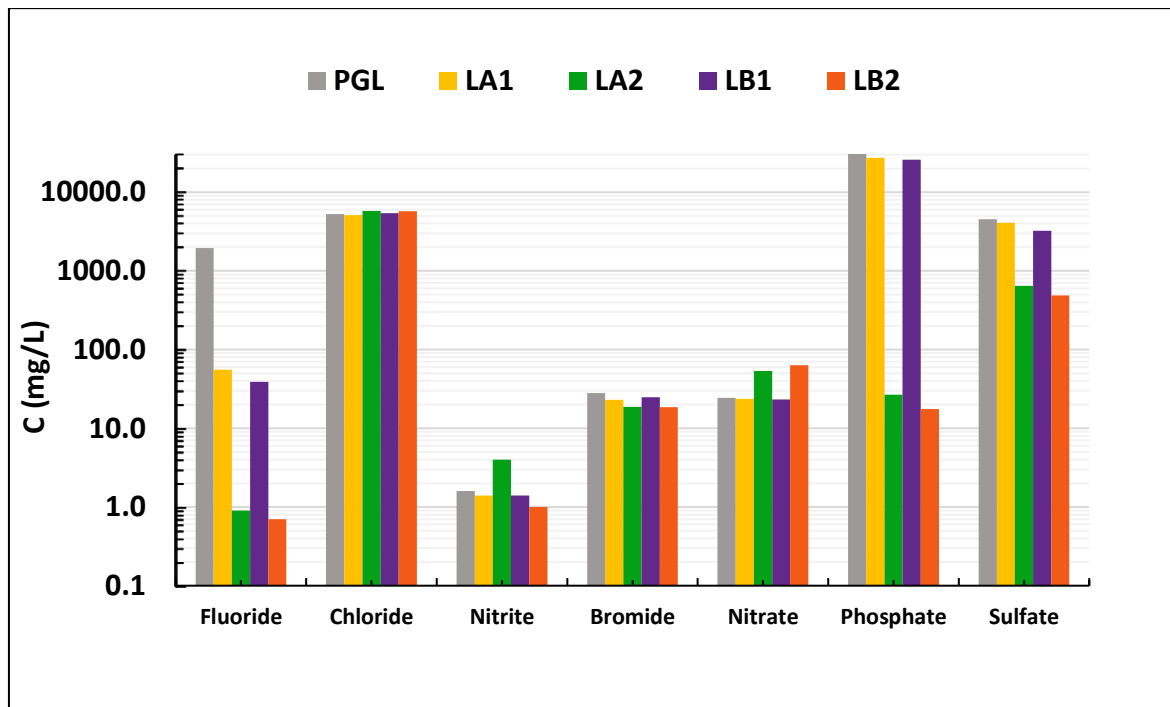


**Figure 10:** Anion concentration (mg/L) of PGL and liquid fraction measured by ion chromatography.

Regarding with the behavior of natural radionuclides, especially  $^{210}\text{Po}$  and U-isotopes ( $^{238-234}\text{U}$ ), during both steps of the neutralization treatment, it can be seen in **Table 3**.

First of all, it can be observed that all natural radionuclides decreased their concentration in both processes and in both steps, as it was the central objective of the cleaning method, to reduce the concentration of contaminants including the radionuclides. The  $^{210}\text{Po}$  activity concentration decreases to a valor of  $6.6 \pm 0.2$  mBq/L in step 1 when  $\text{CaCO}_3$  is used, while with  $\text{Ca}(\text{OH})_2$  the concentration is  $0.2 \pm 0.04$  mBq/L, that is to say the hydrated lime has a better efficiency in the removal of radionuclides. On the other hand, the final concentration of  $^{210}\text{Po}$  obtained in phase 2 of both processes, where  $\text{Ca}(\text{OH})_2$  was used, is essentially the detection limit ( $0.01 \pm 0.02$  mBq/L).

In relation with the  $^{238-234}\text{U}$  activity concentration, the obtained results in the neutralization treatment are in the same line. When  $\text{CaCO}_3$  is used in phase 1, the activity concentration of these isotopes is  $38.8 \pm 1.1$  mBq/L and  $39.6 \pm 1.2$  mBq/L for  $^{234}\text{U}$  and  $^{238}\text{U}$ , respectively, in LA1, while in the case of  $\text{Ca}(\text{OH})_2$  the activity concentration is  $10.2 \pm 0.3$  mBq/L and  $10.1 \pm 0.3$  mBq/L, respectively. In addition, the  $^{238-234}\text{U}$  activity concentration obtained as a final in step 2 of process A is slightly



lower (1 magnitude order) than that obtained with process B, but both of them are really negligible.

To summarize these points, it is important to highlight that the activity concentration of natural radionuclides have been reduced as a consequence of the cleaning process.

Liquid fraction					
Isotope	PGL	Process A		Process B	
		LA1	LA2	LB1	LB2
Po-210	39 ± 0.2	6.6 ± 0.2	0.01 ± 0.02	0.2 ± 0.04	0.01 ± 0.03
U-234	248 ± 12	38.8 ± 1.1	0.02 ± 0.01	10.2 ± 0.3	0.10 ± 0.02
U-238	254 ± 12	39.6 ± 1.2	0.01 ± 0.01	10.1 ± 0.3	0.10 ± 0.02

**Table 3:** Activity concentrations (mBq/L) of PGL and the liquid fractions obtained in the neutralization process measured by alpha- spectrometry.

### 3.1.2. Solid fraction

During the neutralization treatment, different mass amounts of precipitated solid were obtained for each phase and process. In **Table 4**, the mass of formed solid and the alkaline reactive mass per litter of leachate treated are indicated, in order to be possible to calculate the element concentrations and material balances. It is remarkable the increase of mass formed during the second phases of both processes, which is mainly attributed to the phosphate precipitation, as it is expected from the composition of PGL, presenting more than 10 g/L of PO<sub>4</sub>.

Solid fraction				
Mass	Process A		Process B	
	SA1	SA2	SB1	SB2
Solid mass (g/L)	7.8	60.2	11.0	55.3
Alkaline reactive mass (g/L)	13.5	28.6	10.5	26.0

**Table 4:** Solid and reactive mass.

The solid samples have been measured by ICP-MS, XRF, XRD and alpha-spectrometry and the results are developed in this section.

To begin with the discussion, the main elements in the solid fraction are plotted in **Figures 11** and **12**.

As may be seen, solids from both processes contain high proportion of Ca and P, in the quantity of 26.5%; 25.7 % of Ca in step 1 of process A and B, respectively and 7.2%; 6.7 % of P, also in step 1. As it is expectable, the content of F is also high,



since at the pH reached in this stage the fluorides contained in the PGL precipitate with the calcium added. The F concentration has a value in the solid formed of 18.8% in process A and 13.6% in process B, as it can be seen in the figure.

In addition, other elements such as Fe (1.6%; 1.3 %), Na (0.7%; 0.3%) and Mg (0.5%; 0.25%) are also presented in phase 1 of process A and B, respectively.

The principal differences between the processes in step 1 is the S content, since it is noticed that the solid formed in process A (SA1) with  $\text{CaCO}_3$  barely contains S while in process SB1 with  $\text{Ca}(\text{OH})_2$  the quantity of S in the solid is up to 6 times more.

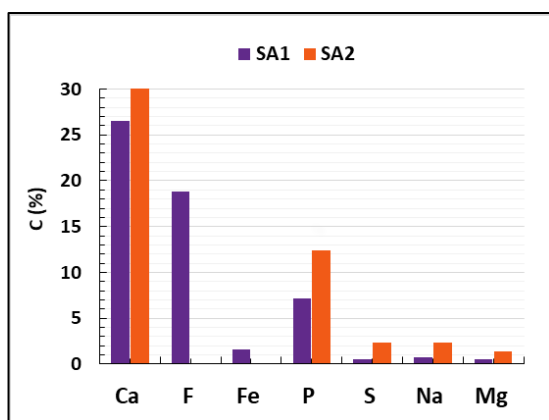


**Figure 11:** Elemental composition (%) of main elements in solids from process A.

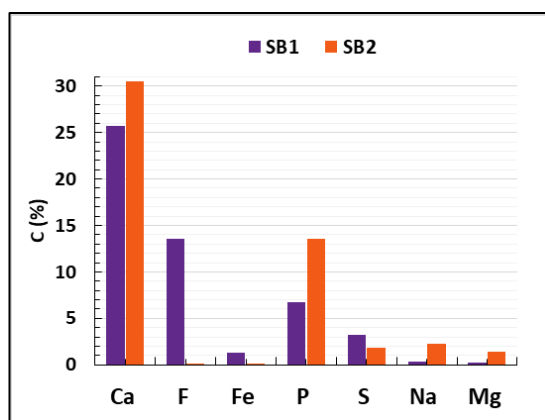


**Figure 12:** Elemental composition (%) of main elements in solids from process B.

Second, there are other elements in minor concentration in the solids from step 1 such as Cd (71.7, 65.5 ppm), Cr (2115, 1680 ppm), Mn (118, 119 ppm), Ni (5.9, 2.6 ppm), Zn (1999, 2000 ppm), As (133, 95.3 ppm), Sr (1000, 1000 ppm), Cu (458, 385 ppm), Pb (44.1, 66.4 ppm) and U (1820, 1500 ppm) in process A and B, respectively.

These elements were plotted in **Figure 13** and **14**. The rest of the elements were in proportion lower than 0.01%.

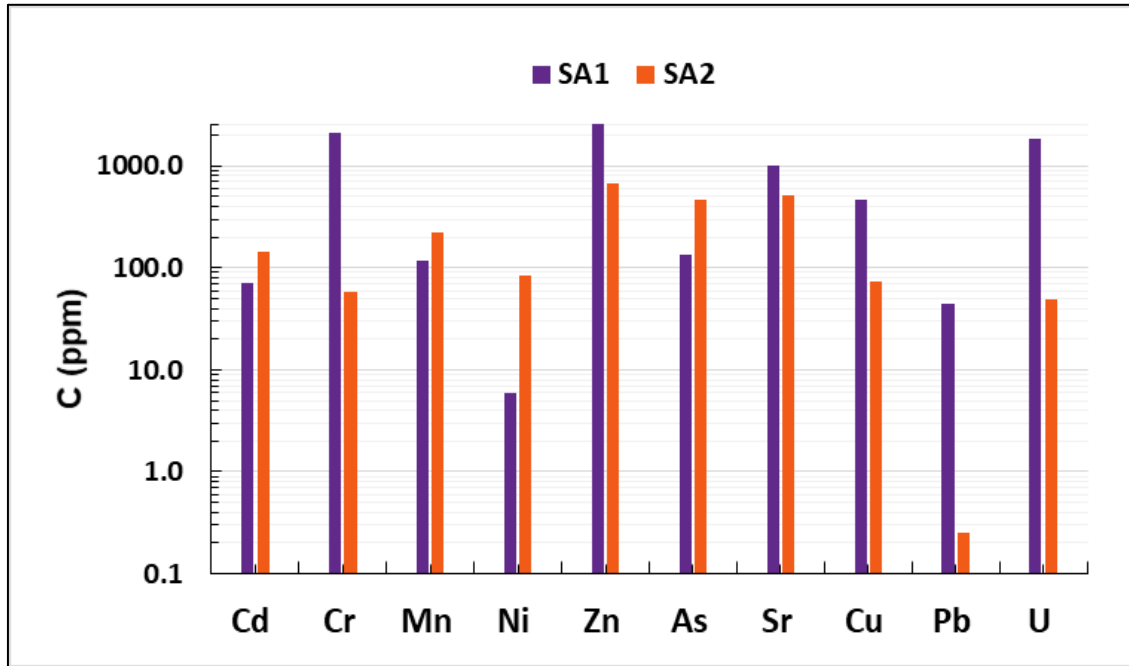


Figure 13: Elemental composition (ppm) of minor elements in solids obtained in process A.

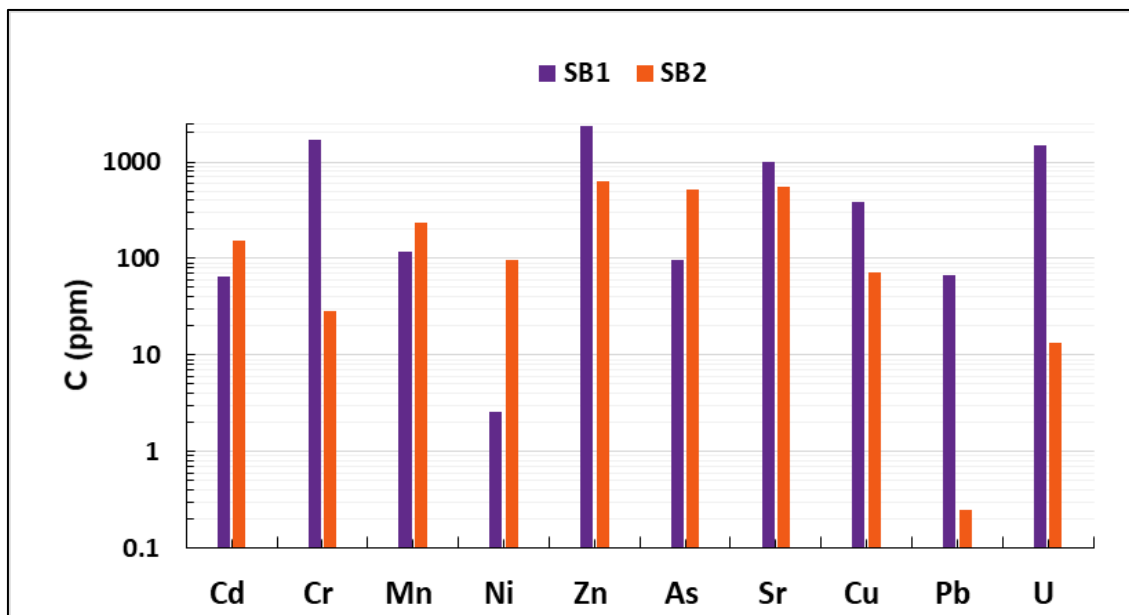


Figure 14: Elemental composition (ppm) of minor elements in solids obtained in process B.

Additionally, many mineral phases have been found in the solids depending on the pH reached in the neutralization treatment. These crystalline phases can be seen in the diffractograms of the samples, which are shown in **Annexe 6.2 and 6.3**, in which the proportion of the minerals as well as the amorphous fractions are indicated.

The formed solid during the neutralization with  $\text{CaCO}_3$  at  $\text{pH} = 3.5$  (Phase SA1), contains  $55.4 \pm 0.9 \%$  of fluorite ( $\text{CaF}_2$ ) and  $44.6 \pm 0.9 \%$  of amorphous content,



while in phase SB1, when  $\text{Ca}(\text{OH})_2$  is used, the content of fluorite is lower ( $36.8 \pm 0.9$ ) and besides  $10.9 \pm 0.5\%$  of gypsum ( $\text{CaSO}_4 \cdot 2\text{H}_2\text{O}$ ),  $9.5 \pm 0.6\%$  of brushite ( $\text{CaHPO}_4 \cdot 2\text{H}_2\text{O}$ ) and  $1.9 \pm 0.4\%$  of ardealite ( $\text{Ca}_2(\text{SO}_4)(\text{HPO}_4) \cdot 4\text{H}_2\text{O}$ ) is formed, with  $41.0 \pm 0.1\%$  of amorphous content. These values are plotted in **Figure 15**.

Taking into account the results from XRF presented in the figures, the concentration of F ( $18.8\%$ ;  $13.6\%$ ), in SA1 and SB1 respectively, indicates that practically all the F content is in form of  $\text{CaF}_2$ . Regarding with Ca concentration, it matches the values obtained in the DRX, which means that calcium is in the form of fluorite in SA1 and in case of SB1, it is forming also gypsum, brushite and ardealite.

In case of solid from process A, there is any mineral compound of P, so it can be notice that all the P is in the amorphous content in the diffractograms of XRD.

Considering that there is no presence of Fe, Na, and Mg in the compounds obtained by XRD in both processes, it can be concluded that these elements are also in the amorphous fraction in the XRD test.

Regarding with solids from second phase, the content of Ca and P is  $31.3\%$ ;  $30.5\%$  and  $12.4\%$ ;  $13.6\%$  of Ca and P, respectively, for process A and B, which is expected since the high content of calcium phosphates precipitated from the PGL due to the increase of pH because of the addition of calcium in form of  $\text{Ca}(\text{OH})_2$  during the neutralization.

It is observed that the concentrations of elements such as F ( $<0.01\%$ ) and Fe ( $<0.04\%$ ) are in a value near the LoD of the technique in stage 2, and on the other hand, elements such as S ( $2.3$ ;  $1.8\%$ ), Mg ( $1.4\%$ ), Na ( $2.4$ - $2.3\%$ ) and P ( $12.4$ - $13.6\%$ ) has a concentration 3 times higher than solid of step 1 in both processes, with exception of S in process B, which has a value of  $1.8\%$  (near a half than solid step 1). This means that part of the amorphous content is constituted by compounds of these elements and additionally solids from phase 2 of both processes contain 3 times higher of Mg, Na and P than solids from step 1.

Also, Ni ( $83.3$ ;  $97.0$  ppm), Cd ( $141$ ;  $154$  ppm), Mn ( $222$ ;  $232$  ppm) and As ( $465$ ;  $518$  ppm) precipitate in second step of both processes in around 80-90% higher than concentration of step 1. On contrary, Pb ( $<0.5$  ppm) is practically eliminated in step 1, as it was seen in the liquid fraction, so this element does not precipitate in this step, since it has already precipitated completely in step 1.

Regarding with other minor elements, such as Cr ( $58$ ;  $29$  ppm), Zn ( $100$  ppm), Sr ( $509$ ;  $553$  ppm) and Cu ( $72.6$ ;  $72.1$  ppm), it is notable than they are in concentrations





near a half than concentration of these metals in step 1, since they precipitate in higher quantity in lower pH.

In relation with mineral compounds of solids from second phase, it can be seen that corresponds to Hydroxylapatite (HA) which it is a compound of calcium phosphate ( $\text{Ca}_5(\text{PO}_4)_3\text{OH}$ ) and it is presented in the solid in  $81.8 \pm 0.7 \%$  with  $18.2 \pm 0.8 \%$  of amorphous content in process A. In process B, the percentage is lower ( $76.9 \pm 0.6\%$  of HA with  $23.2 \pm 0.6 \%$  amorphous content), what is a factor to take into account when the objective is to obtain a waste with probabilities of valorization, intending to generate the most quantity possible of waste with a high purity. These concentrations can be seen plotted in **Figure 15**.

The correlation between both techniques, XRF and XRD, indicates that there is 15.3%; 13.3% of Ca as amorphous in solid SA2 and SB2, respectively. Additionally, a part of the content of P is also as amorphous, about 8.7% in process A and 10.6% in process B, which means that probably there is amorphous phase of HA, however it need to be analyze with other techniques.

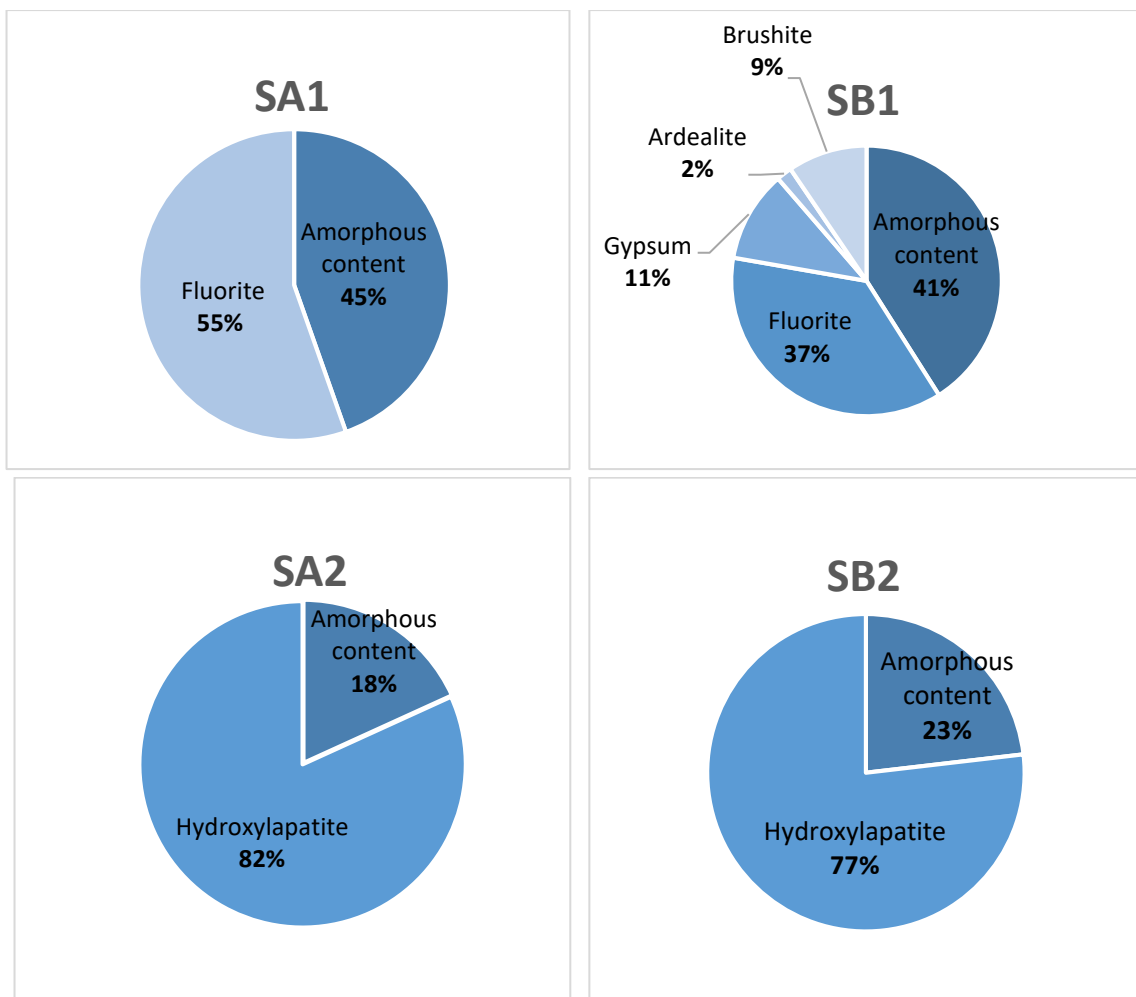


Figure 15: Mineral composition of solids formed after neutralization treatment measured by XRD.



To summarize the characterization of the solid wastes presented in this section, the correlation between the values of metals concentration for a typical soil and those of the solids wastes are presented in the **Table 5**. As it can be seen, the solids from first step contain in order of 200-300 times of F, 500-600 times of U, 800 times of Cd and around of 20-50 times of P, As, Cr and Cu than a typical soil. Moreover, solids of step 2 contain 1600-1700 times of Cd and approximately 100 times more of As.

		Process A		Process B	
Typical soil		SA1	SA2	SB1	SB2
Al (%)	15.4	$9.1 \cdot 10^{-3}$	$6.5 \cdot 10^{-4}$	$5.2 \cdot 10^{-3}$	$6.5 \cdot 10^{-4}$
Ca (%)	3.56	7.4	8.7	7.2	8.5
F (%)	0.06	$3.4 \cdot 10^2$	$1.8 \cdot 10^{-1}$	$2.4 \cdot 10^2$	$1.8 \cdot 10^{-1}$
Fe (%)	5	$3.2 \cdot 10^{-1}$	$7.9 \cdot 10^{-3}$	$2.6 \cdot 10^{-1}$	$7.9 \cdot 10^{-3}$
K (%)	2.8	$7.1 \cdot 10^{-2}$	$4.3 \cdot 10^{-2}$	$3.6 \cdot 10^{-2}$	$5.4 \cdot 10^{-2}$
Mg (%)	2.5	$2 \cdot 10^{-1}$	$5.6 \cdot 10^{-1}$	$1.0 \cdot 10^{-1}$	$5.6 \cdot 10^{-1}$
Na (%)	3.3	$2.1 \cdot 10^{-1}$	$7.3 \cdot 10^{-1}$	$1.0 \cdot 10^{-1}$	$7.0 \cdot 10^{-1}$
P (%)	0.15	$4.8 \cdot 10^1$	$8.3 \cdot 10^1$	$4.5 \cdot 10^1$	$9.1 \cdot 10^1$
S (%)	0.01	$8.1 \cdot 10^1$	$3.7 \cdot 10^2$	$5.2 \cdot 10^2$	$2.9 \cdot 10^2$
Si (%)	66.6	$3 \cdot 10^{-4}$	$1.6 \cdot 10^{-2}$	$3.0 \cdot 10^{-4}$	$1.6 \cdot 10^{-2}$
Zn (%)	0.01	$3.1 \cdot 10^1$	$1.2 \cdot 10^1$	$3.0 \cdot 10^1$	$1.2 \cdot 10^1$
Cd (ppm)	0.09	$8 \cdot 10^2$	$1.6 \cdot 10^3$	$7.3 \cdot 10^3$	$1.7 \cdot 10^3$
As (ppm)	4.8	$2.8 \cdot 10^1$	$9.7 \cdot 10^1$	$2 \cdot 10^1$	$1.1 \cdot 10^2$
Cr (ppm)	92	$2.3 \cdot 10^1$	$6.4 \cdot 10^{-1}$	$1.8 \cdot 10^1$	$3.2 \cdot 10^{-1}$
Cu (ppm)	28	$1.6 \cdot 10^1$	2.6	$1.4 \cdot 10^1$	2.6
Ni (ppm)	47.00	$1.2 \cdot 10^{-1}$	1.8	$5.5 \cdot 10^{-2}$	2.1
Pb (ppm)	17.00	2.6	$2.9 \cdot 10^{-2}$	3.9	$2.9 \cdot 10^{-2}$
Sr (ppm)	320.00	3.1	1.6	3.1	1.7
U (ppm)	2.70	$6.7 \cdot 10^2$	$1.8 \cdot 10^1$	$5.6 \cdot 10^2$	5

**Table 5:** Waste/Typical Soil relation for metals (elevated grade of contamination in red).

The activity concentrations of  $^{234-238}\text{U}$  and  $^{210}\text{Po}$  found in the generated solids during both neutralization processes are indicated in **Table 6**.

As it can be seen, the highest activity concentrations of both radionuclides are founded in the solid from stage 1 (SA1 and SB1), being  $25900 \pm 418$  Bq/kg of  $^{234-238}\text{U}$  and  $5120 \pm 83$  Bq/kg of  $^{210}\text{Po}$  in solid from process A and  $20600 \pm 570$  Bq/kg of  $^{234-238}\text{U}$  and  $4370 \pm 136$  Bq/kg of  $^{210}\text{Po}$  in solid from process B. They decrease (in around 95-97%) in the following step when the pH increases. Nevertheless, the activity concentration of both radionuclides in all solids are very high, exceeding up to 3 orders of magnitude the worldwide median value for natural soils (35 Bq/kg)



(UNSCEAR, 2000). The principal difference between the processes is that the solid obtained in step 2 of process B (SB2) has 27% lower of <sup>210</sup>Po concentration and 28% lower than <sup>234-238</sup>U.

Solid fraction				
Isotope	Process A		Process B	
	SA1	SA2	SB1	SB2
	A (mBq/g)	A (mBq/g)	A (mBq/g)	A (mBq/g)
Po-210	5100 ± 80	60 ± 4.7	4400 ± 130	20 ± 0.6
U-234	25900 ± 400	750 ± 18	20600 ± 600	200 ± 7.1
U-238	25900 ± 400	760 ± 18	20600 ± 600	220 ± 7.1

Table 6: Radiological characterization of solid fraction measured by alpha- spectrometry.

### 3.1.2 Precipitation efficiencies

In order to determine the proportion of contaminants removed in all cases, the material balances were done. In **Figure 16** it is explained the compartments considered during the mass balances, being  $V_0$  the initial volume of PGL to be cleaned,  $V_1$  the volume of liquid obtained after step 1 of neutralization process and  $m_1$  the mass of solid generated in step 1. In concordance,  $V_2$  is the volume of liquid obtained in phase 2 and  $m_2$  the mass of solid from that phase. The percentage of precipitation of an element (x) during the process or "Precipitation Efficiency" (PE), is defined as the relationship between the amount of an element in the resulting solid (1 minus the dissolved remaining fraction) and the amount of that element in the initial solution. Thus, the precipitation efficiency of a certain element (x) is determined according to the following equation:

$$PE (\%) = \left( 1 - \frac{C_{1,2} \cdot V_{1,2}}{C_i \cdot V_i} \right) \cdot 100 \quad \text{Eq. 4}$$

Where  $C_i$  (mg/L) is the concentration of the element in the initial solution "i",  $C_{ij}$  (mg/L) is the concentration of the element in the final solution,  $V_{ij}$  (L) is the final volume of the effluent, and  $V_i$  (L) is the volume of the initial solution, being "j" = 1 or 2, depending on the step.

In the case of Ca, the added amounts of  $\text{CaCO}_3$  or  $\text{Ca(OH)}_2$  were considered. Thus, the precipitation efficiencies for Ca are calculated with the following equation, where "mi added" is the amount (mg) of Ca added:

$$PE (\%) = \left( 1 - \frac{C_{1,2} \cdot V_{1,2}}{C_i \cdot V_i + m_{i \text{ added}}} \right) \cdot 100 \quad \text{Eq. 5}$$

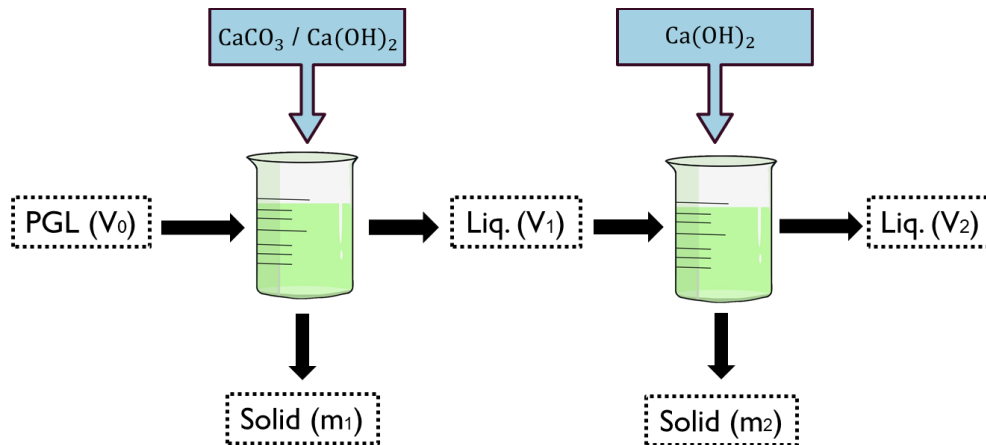


Figure 16: Scheme of fractions obtained in the experiments.

In **Figures 17** and **18** are plotted the outcomes from the step 1 of processes. As it can be seen, from the 100% of PGL that enter in the process, the line out is constituted by the solid ( $m_1$  or SA1/SB1) and the liquid ( $V_1$  or LA1/LB1).

There are elements such as Al (87; 88%), Cr (85; 92%), Fe (99; 100%), Pb (99; 100%) and Zn (83; 96%) that are mainly transferred to the solid during the step 1 in percentages around 80; 100%, while other elements such as Ca (37; 50%), Cu (42; 50%), P (23; 28%), Sr (22; 27%) and U (35; 45%) are removed in percentages around 20-45%. Besides, there are other very conservative elements such as As (9, 11%), Cd (12, 16%), Mg (9, 8%), Mn (4, 3%) and Ni (9, 16%) that have a transfer percentage lower than 20% into the solid in phase 1.

The principal differences between process A and B are the behavior of Cu, S, Zn and U. When  $\text{Ca(OH)}_2$  is used as an alkaline reactive in the step 1 of the process, it is possible to obtain a solid with 8% more of Cu, 22% more of S, 13% more of Zn and 10% of U, which means that the effluent has less concentration of these elements in phase 1 of process B, representing the most interesting result the lower concentration of U possible to obtained in step 1 of process A, with  $\text{CaCO}_3$ .

Moreover, there are some elements that their precipitation is higher with  $\text{Ca(OH)}_2$  comparing with  $\text{CaCO}_3$ , such as As (3%), Cd (4%), Ni (8%), P(5%), Si(4%) and Sr (5%), obtaining solids with slight differences.

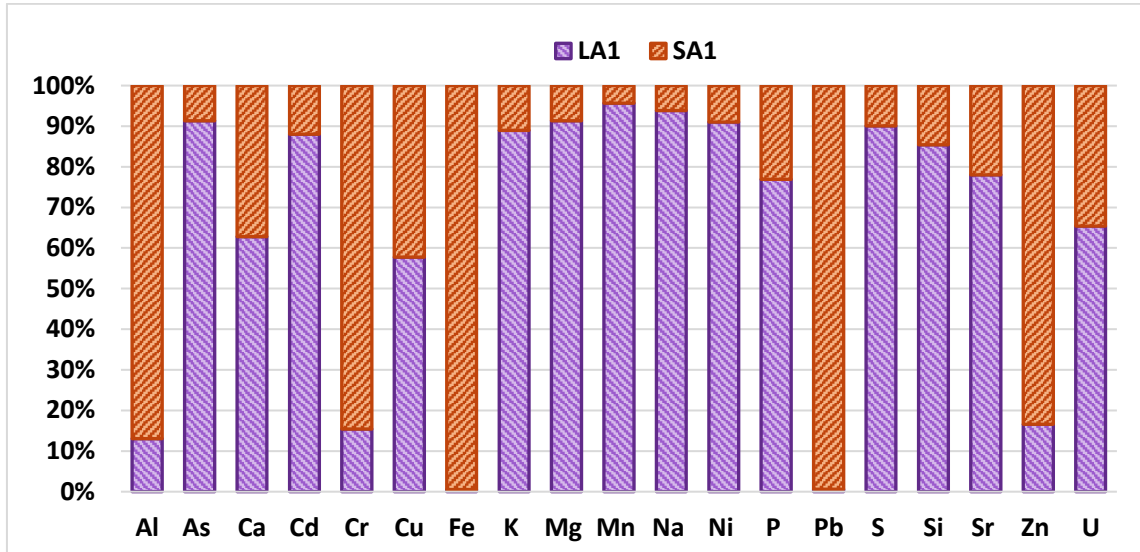


Figure 17: Material balance of step 1 of process A.

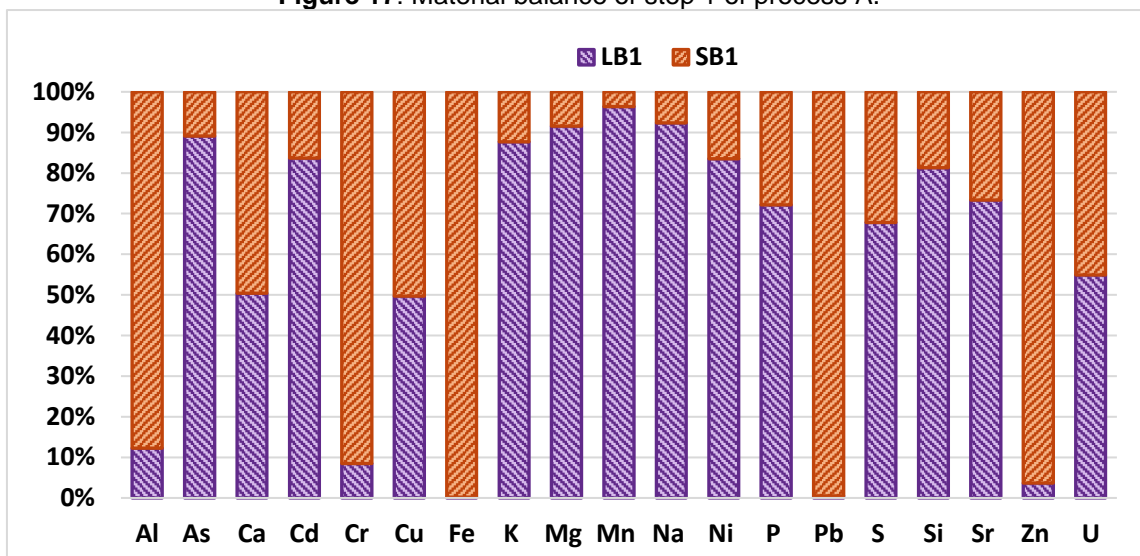


Figure 18: Material balance of step 1 of process B.

In **Figures 19** and **20** are shown the balances of the complete processes. As it can be seen, from the 100% of PGL that enter in the process, the line out is constituted by the solids from both sequential steps ( $m_1$  or SA1/SB1) and ( $m_2$  or SA2/SB2) and the final cleaned liquid ( $V_2$  or LA2/LB2), since  $V_1$  is consider a mid-come between both steps of the process.

In the figures it can be notice that the results from process A and B are similar, being the principal differences founded in step 1 of both processes, since the different reagent used. As a major conclusion, from the 100% of PGL consider as an income of the processes, there are elements such as Al (87; 87%), Cr (85; 92%), Fe (99; 99%), Pb (99; 100%) and Zn (83; 96%) that are transferred to solids in step 1 in transfer percentages of 80-100%, while elements such as As (9; 11%), Cd (12; 16%), Mg (9; 8%), Mn (4; 4%), Ni (9; 16%), P (23; 28%), S (10; 32%), Si (15; 19%)



and Sr (22; 27%) are transferred to solids in first step in percentages lower than 30%.

In case of solids at step 2 of both processes, the situation is in concordance, since those elements such as As (100%), Cd (100%), Mg (99; 100%), Mn (100%), Ni (97; 96%), P (99%), S (88; 87%), Si (99%) and Sr (97; 98%) are transferred to solids of step 2 in percentages higher than 87%.

Finally, there are elements such as K and Na that are not affected by the sequential neutralization process, remaining in the final liquid obtained in percentage of transference higher than 60%, while the rest of the elements passes to solids at step 1 or 2.

Regarding with the transfer percentage in the liquid final flow, it can be noticed that it is negligible (lower than 1-1.5%) for toxic elements such as As (0%), Ca (0.8%), Cd (0%), Cr (0.6; 1.2%), Mg (0.1; 0%), Mn (0%), P (0.1%), Si (0.7%), Ni (2.8; 3.1%) and U (0%), occurring only transference of Al (25; 27%), Cu (1.4; 1.7%), Fe (5.3; 13%), K (67; 63%), Na (62; 64%), Pb (7.5; 9.7%), S (12; 13%), Sr (2.5; 2.3%) and Zn (1.0; 4.8%), in process A and B, respectively.

The principal differences between both processes are the higher percentage that remains in dissolution in the final liquid of metals as Al (2%), Fe (8%), Na (2%), Pb (3%) and Zn (4%) in process B respect process A, which means that in process A it is possible to obtain an effluent cleaner regarding with concentration of that metals.

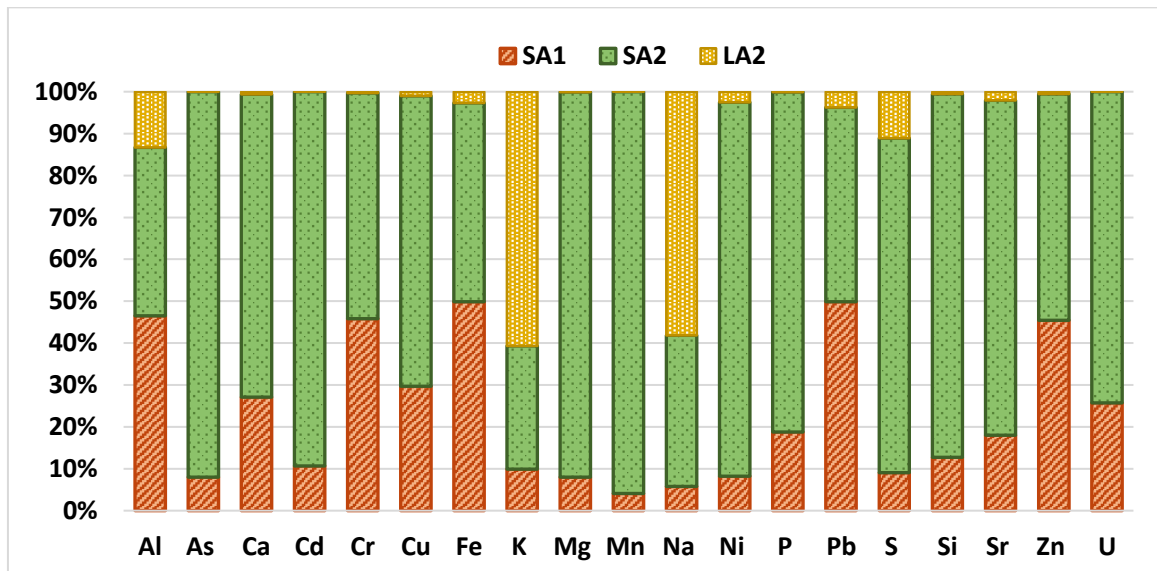


Figure 19: Material balance complete process A.

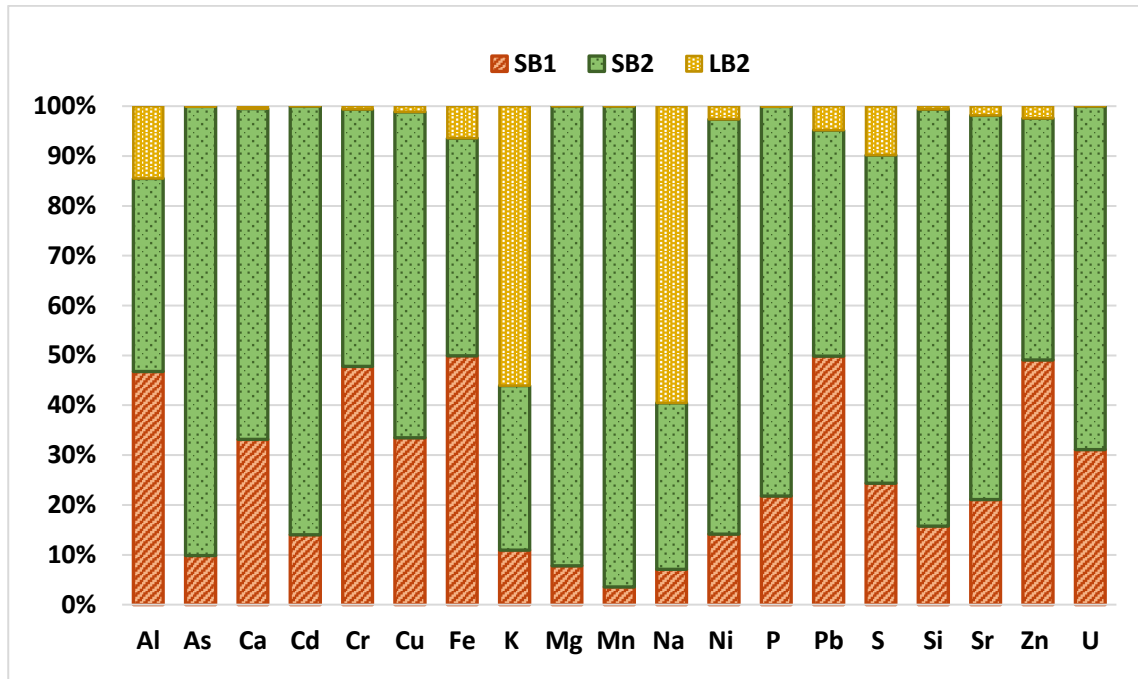


Figure 20: Material balance of complete process B.

The exact values of precipitation percentages and the concentration of each element in the steps of both processes are shown in **Annexes 6.5 and 6.6**. The standard uncertainty of the material balances was estimated for all elements around 10-15%, except for the case of Al, Fe and Si in which the error is higher. This fact can be attributed to the trace elements that contain the alkaline reagents used, especially in the case of  $\text{Ca}(\text{OH})_2$ . The reagents used were measured by ICP-MS in order to determine the trace elements content and therefore corrections were applied. This data can be found in **Annexe 6.7**.

## 3.2 Environmental Implications

### 3.2.1 Liquid discharge limits in Andalusia

In the Andalusia Region, the discharge of the liquid effluents into coastal waters is controlled by Decreto 109/2015 (2015), which approves the regulation of discharges to the Hydraulic Public Domain and the Maritime-Terrestrial Public Domain of Andalusia, in which is established the emission limit value for certain parameters such as phosphates, fluorides, chrome, cadmium, aluminum, arsenic, and other metals, as it can be seen in **Table 7**.

The final effluent obtained as a result of the sequential neutralization process in final phase of both treatments was also incorporated in **Table 7**. As it can be noticed, the composition of the effluent using  $\text{CaCO}_3$  and  $\text{Ca}(\text{OH})_2$  comply all set out requirements for concentrations of discharge ( $\text{Al} < 10 \text{ mg/L}$ ,  $\text{As} < 1.2 \text{ mg/L}$ ,  $\text{Cd} <$





0.04 mg/L, Cr < 0.33 mg/L, Cu < 0.9 mg/L, Mn < 9 mg/L, Ni < 0.66 mg/L, P < 55mg/L, Pb < 0.26 mg/L and Zn < 1.8 mg/L). In addition, the fluorides, nitrates and phosphates are under the limit, while F<sup>-</sup> <17 mg/L, NO<sub>3</sub><sup>-</sup> < 110 mg/L and PO<sub>4</sub><sup>-</sup> <165 mg/L. The only exception is the requirements for the pH because the pH reached in final step is up to 12. For this reason, it is necessary to study a treatment in order to decrease the effluent pH and to possibilities the discharge of these liquid effluents into coastal waters. The kind of treatments that is actually use for increase pH of effluent waters is CO<sub>2</sub> injection, and need to be studied in depth in future research.

Element	Process		Limit value Decreto 109/2015 (mg/L)
	A2	B2	
	C (mg/L)	C (mg/L)	
Al	0.3	0.3	10
As	<0.01	<0.01	1.2
Ca	213	180	-
Cd	<0.01	<0.01	0.04
Cr	<0,1	<0,1	0.33
Cu	0.1	0.1	0.9
Fe	<0,1	<0,1	-
K	227	204	-
Mg	0.7	<0,1	-
Mn	<0,1	<0,1	9
Na	4030	4020	-
Ni	0.2	0.2	0.66
P	8.7	5.7	55
Pb	<0,1	<0,1	0.26
S	236	184	-
Si	4.1	4.3	-
Sr	1.3	1.1	-
U	<0,1	<0,1	-
Zn	<0,1	<0,1	1.8
<b>Anions</b>			
F <sup>-</sup>	0.9	0.7	17
Cl <sup>-</sup>	5770	5750	-
Br <sup>-</sup>	18.7	18.6	-
NO <sub>3</sub> <sup>-</sup>	53.3	63.4	110
PO <sub>4</sub> <sup>-</sup>	26.7	17.5	165
SO <sub>4</sub> <sup>-</sup>	645	488	-
pH	12	12	9.5-5.5

Table 7: Final effluent obtained and its comparison with limit values (Decreto 109/2015).



### 3.2.2 Landfill disposal admission

The European Commission regulates disposal waste in landfill by Directive 1999/31/CE, and the waste acceptance criteria are established for each class of landfill in Directive UNE-EN 12457-4. The leaching test is done with the purpose of evaluate the performance of each element regarding with their mobility, concentration and transfer factor, in order to determine the landfill disposal.

The results of Leaching Test are shown in **Table 8**. As it can be seen, there are concentrations of certain elements that are similar in step 1 of both processes such as As (21.9; 18.6 mg/kg), Cd (2.2; 1.6 mg/kg), Mg (573; 525 mg/kg), Mn (8.7; 8.9 mg/kg), Ni (2.8; 2.2 mg/kg), P (7200; 7230 mg/kg), Ti (0.1 mg/kg) and V (1.0; 0.7 mg/kg) in process A and B, respectively.

When it is used  $\text{CaCO}_3$  (process A) there is lower release of contaminants such as Al (4 mg/kg), Ca (4190 mg/kg), S (1560 mg/kg) and Sr (22.5 mg/kg), comparing with process B where the concentration of these elements are Al (6.8 mg/kg), Ca (9280 mg/kg), S (4930 mg/kg), and Sr (36.8 mg/kg) but on the contrary, there are a higher content of K (705 mg/kg) instead of 218 mg/kg, Na (2700 mg/kg) in place of 1390 mg/kg and Zn (57.4 mg/kg) rather than 26.1 mg/kg in process A.

Regarding with concentrations obtained from solid leachates of second phases, it can be seen that they are lower than steps 1. There are elements with similar behavior in both processes such as Al (1.0 mg/kg), Cd (1.0 mg/kg), Cr (0.3; 0.1 mg/kg), Cu (0.1; 0.05 mg/kg); Mn (1.0 mg/kg), Ni (0.3 mg/kg), Sr (0.3; 0.1 mg/kg), Ti (0.04 mg/kg), V (0.1; 0.3 mg/kg) and Zn (0.01; 0.02 mg/kg).

The second phase is the final result of the neutralization process and the one for evaluation into final disposal. Regarding with this, the waste obtained in process B, has 3 times lower of Ca, (31.3 mg/kg instead of 90.3 mg/kg in process A), 68% lower Mg (328 mg/kg rather than 466 mg/kg), 26% lower Na (8630 mg/kg in place of 11660 mg/kg) and 12% lower S (4620 mg/kg in contrast with 5200 mg/kg in process A) but it has seven times more of P (544 mg/kg while solid leachate A has 78.2 mg/kg).

The most interest result is that in process A, it is possible to obtain an As concentration 75% lower than in the case of neutralization with  $\text{Ca(OH)}_2$  and because of this, the waste can be consider as hazardous waste taking into account the limits from Decreto 646/2020 which gives parameters for Landfill disposal.

Moreover, regarding with the As release from process B, the generated waste cannot be dispose in a landfill, since it outpoints the limit for “hazardous waste”. It is necessary additional research to determine the behavior of this contaminant and



final disposal. Although, in case of valorization of the solid fraction accomplish with check that the final destination of the waste complies with the regulations of its use.

Regarding with the established limits of other contaminants, they have concentrations lower than those established for “no hazardous wastes”.

Element	Process A		Process B		Inert Waste	No Hazardous waste	Hazardous waste
	A1	A2	B1	B2			
	Concentration (mg/kg)						
Al	4.0 (0.4)	1.0 (0.4)	6.8 (1.0)	1.0 (0.5)			
As	21.9 (16.5)	8.2 (1.7)	18.6 (19.6)	32.6 (6.3)	0.5	2	25
Ca	4190 (1.6)	90.3 (0.03)	9280 (3.6)	31.3 (0.01)			
Cd	2.2 (3.0)	1.0 (0.7)	1.6 (2.4)	1.0 (0.7)	0.04	1	5
Cr	0.2 (0.01)	0.3 (0.6)	0.05 (0.003)	0.1 (0.4)	0.5	10	70
Cu	2.3 (0.6)	0.1 (0.1)	1.3 (0.4)	0.05 (0.02)	2	50	100
K	705 (29.9)	869 (71.2)	218 (18.2)	911 (59.0)			
Mg	573 (9.8)	466 (3.1)	525 (17.8)	328 (1.9)			
Mn	8.7 (7.4)	1.0 (0.4)	8.9 (7.5)	1.0 (0.4)			
Na	2700 (43.1)	11660 (61.0)	1390 (48.6)	8630 (45.4)			
Ni	2.8 (47.5)	0.3 (0.3)	2.2 (84.9)	0.3 (0.4)	0.4	10	40
P	7200 (9.9)	78.2 (0.1)	7230 (10.7)	544 (0.4)			
S	1560 (31.7)	5200 (23.3)	4930 (15.8)	4620 (26.1)			
Sr	22.5 (2.8)	0.3 (0.1)	36.8 (5.7)	0.1 (0.02)			
Ti	0.1 (5.1)	0.04 (3.0)	0.1 (4.5)	0.04 (2.8)			
V	1.0 (0.03)	0.1 (0.5)	0.7 (0.03)	0.3 (1.6)			
Zn	57.4 (2.3)	0.01 (0.002)	26.1 (1.1)	0.02 (0.003)	4	50	200

**Table 8:** Concentration (mg/kg) and transfer factor (%) (in parentheses, with red the high values) obtained after leaching test of samples and its comparison with Decreto 646/2020 (Landfill disposal Regulations).

The values of transfer factor are presented in **Table 8**, as can be observed, there are elements more mobile such as As (16.5%-19.6%), K (29.9%-18.2%), Mg (9.8%-17.8%), Na (43.1%-48.6%), Ni (47.5%-84.9%), P (9.9%-10.7%) and S (31.7%-15.8%) in step 1 of process A and B, respectively, being K and S more mobile in process A (with CaCO<sub>3</sub>) and Ni in process B (with Ca(OH)<sub>2</sub>), regarding with the concentration.

But to point out the importance of the final step of the processes, only elements as K (71; 59%) and Na (61; 45%) have a high transfer factor, which are the conservative elements that were not affected by the neutralization sequential process, while the rest of the elements has a transfer factor lower than 5% in the second step of the cleaning processes, with exception of S with has a TF of 23; 26%, in process A and B, respectively.



In relation with the activity concentration of natural radionuclides after Leaching Test, they were measured by alpha-spectrometry and the results are shown in **Table 9**. As it can be appreciated, the concentrations of  $^{210}\text{Po}$  and  $^{234-238}\text{U}$  are really low, similar with seawater concentrations, as it has  $0.004 \pm 0.0004$  mBq/L of  $^{210}\text{Po}$  and  $0.04 \pm 0.002$  mBq/L of  $^{234-238}\text{U}$  (Guerrero et al., 2021). This means that it is no relevant the radiological impact of the isotopes once the neutralization process was applied and that they can be released into coastal waters.

Leachate samples				
Isotope	Process A		Process B	
	Lix SA1	Lix SA2	Lix SB1	Lix SB2
	A (mBq/L)	A (mBq/L)	A (mBq/L)	A (mBq/L)
Po-210	$0.10 \pm 0.01$	< D.L	$0.10 \pm 0.01$	< D.L
U-234	$0.30 \pm 0.03$	< D.L	$0.30 \pm 0.04$	< D.L
U-238	$0.50 \pm 0.03$	< D.L	$0.10 \pm 0.02$	< D.L

**Table 9:** Natural radionuclides activity of samples obtained after leaching test.

### 3.3 Diagnosis of valorization for the generated wastes

As it was discussed in the previous sections, the generated wastes during PGL treatment could be disposed in a landfill, but the new waste Law 7/2022, of April 8, which focus on prevention, preparation for reuse, recycling and other forms of recovery and considering the challenge of the circular economy, impulse the necessity to recycle and valorize the obtained wastes.

These wastes can have some potential applications in the field of ceramic materials, cement and concrete manufacture. In this section, the most viable options from technical and economic point of view for valorization of the solid wastes are developed, taking into account the comprehensive literature review.

The first solid waste is formed essentially by fluorite (compound of calcium fluoride) and could be valorize as additive in the manufacture of commercial cements and ceramics. The waste obtained in the second step is formed by calcium phosphates (Hydroxylapatite) and could be used as raw material in the manufacture of phosphate fertilizers.

#### 3.4.1 Fluorite

Considering the characterization of these wastes from step 1 and the literature consulted, two possibilities could be raised for the recovery of the fluorite.

Among the construction history, cement was the principal material used for building manufacture. The Portland cement and its derivatives are compounded essentially by limestone, clay and gypsum, which are abundant minerals.



In effect, cement consists on a fine powder obtained by grinding slag from a mixture of clay and limestone. The combination of cement and water produces a plastic mass that progressively hardens, as interlocking crystals of hydrated aluminosilicates are formed, until it reaches a hardness similar to a stone (V. Bonavetti, 1998). When cement is mixed with sand, mortar is obtained and when it is mixed with sand and gravel, concrete is obtained.

Briefly, the cement manufacturing process consists on the following stages (M.F. Carrasco, 2012):

- 1- Mixing of raw materials and obtaining crude cement.
- 2- Crushing and drying of crude cement.
- 3- Grinding and silage of raw cement
- 4- Heating of raw cement or clinkerization
- 5- Cement grinding
- 6- Storage

Chemical composition of Portland clinker consists of four main components: tricalcium silicate ( $C_3S$ ), dicalcium silicate ( $C_2S$ ), tricalcium aluminate ( $C_3A$ ) and tetracalcium ferroaluminate ( $C_4AF$ ). In fact, the silicates found in the clinker are not pure since they contain small amounts of oxides which have important effects on atomic ordering, crystal form, and hydraulic properties of cement.

The alite (impure form of  $C_3S$ ) in the pure clinker occurs as colorless and opaque crystals with a prismatic section. This phase is hydraulically active, presenting a high hydration speed that determines the high initial resistance of the cement while the belite phase (impure form of  $C_2S$ ) presents crystals with a greater luster and a rounded or striated shape. The reaction rate in the belite is slower and releases less total heat, giving the cement long-term resistance. (Maldonado and Carrasco, 2012).

In step 3, before clinkerization, many mineral additions can be added in order to improve the technological performance of cements, either in fresh or hard properties. Many authors have studied the incorporation of calcium fluoride in the clinker for cement elaboration. Moreover, in a study from Wei-Ting Lin; 2019, it has been studied mortar specimens with replacement of cement (0%, 5%, 10%, 15%, 20%, 25%, and 30% based on weight percentage) with calcium fluoride sludge from industrial waste produced in the manufacturing of solar cells. The results indicated that partially replacing cement with calcium fluoride sludge improved the compressive strength, permeability and pore-structure, as well as 10% replacement of cement seems to give superior mechanical properties and durability due to the denser microstructures formed.



Another study from Dominguez et al, 2010, have showed that when certain amount of  $\text{CaF}_2$  is added to the clinkerization process the mechanical properties are modified since the final amount of alite formed ( $\text{Ca}_3\text{SiO}_5$ ) is higher. They concluded that the highest compressive strength was developed with 0.4 wt.% of  $\text{CaF}_2$ , increasing the compressive strength of the clinker paste from 30 MPa to almost 40 MPa. In addition, the evidence from this study suggests that  $\text{CaF}_2$  has a small effect on  $\text{CaCO}_3$  decomposition, on contrary to belite where  $\text{CaF}_2$  has an important effect on their corresponding temperatures. So, as a conclusion, the calcium fluoride acts as a carrier, decreasing the viscosity and surface tension of the oxide melt because it reduces the temperature at which the oxide melt is formed, enabling the alite to form at lower temperature.

Another study about the addition of  $\text{CaF}_2$  in proportion of 0.25, 0.50, and 1% and MgO in 1, 2, and 3% percentages added to a mixture composed from limestone, sand, and loam was conducted by Akin Altun, 1999, in order to improve the raw mix burning, because these materials decrease the formation temperature of the clinker minerals by increasing the calcination, solid-state reaction, melt and alite formation rate. The study concluded that the amount of CaO free decreases with increasing  $\text{CaF}_2$  content. The reason for the CaO free reduction is the increase in the speed of the solid-state reaction due to the easy diffusion effect of fluorine and the acceleration of the necessary reactions for clinker phase formation due to the low-viscosity fluorine melts.

In the research from Dahhou et al, (2021), it was presented a new method to synthesize belite clinkers at even lower temperatures by incorporating the natural fluorite ( $\text{CaF}_2$ ) into a mixture of limestone and alumina sludge originated from water purification plants. The results indicated that the synthesized belite cement possesses mechanical strength similar to that of ordinary belite cement. In addition, the introduction of  $\text{CaF}_2$  into the clinkers not only lowers their preparation temperatures but also facilitates the formation of crystalline phases which eventually leads to improved hydraulic properties of the cement.

Additionally, the second possibility for the waste obtained in step 1 is the manufacture of ceramic tiles from mixtures of a commercial red stoneware mixture (RSM) with different concentrations of waste obtained.

$\text{Li}_2\text{O}-\text{Al}_2\text{O}_3-\text{SiO}_2$  (LAS) based glass-ceramic are widely studied because they own low coefficient of thermal expansion and adjustable crystallization phase, enhancing the reduction of thermal stress and extension of service life. D. Feng, 2016, has studied the effects of  $\text{CaF}_2$  on the LAS based glass-ceramics and glass-ceramic/diamond composites. The addition of  $\text{CaF}_2$  decreased the temperature of refractoriness, because that fluorine entered into glass network and replaced non-



bridge oxygen ions, weakening glass network and relaxing the glass structure. The high temperature fluidity of glass binder is inversely proportional to the value of refractoriness. The study shows the benefits of the addition of calcium fluoride for the glass crystallization and mechanical properties, moreover, when the content of  $\text{CaF}_2$  reached 7 wt.%, the nucleation temperature of the glass-ceramic reduced  $9^\circ\text{C}$  and the bending strength and Rockwell hardness of the glass-ceramic/diamond composites improved 27.68% and 29.08%, respectively.

Further, another study developed by J. Wang et al, 2021 shows ceramic composites based on the addition of nanosized  $\text{CaF}_2$  solid lubricants produced by vacuum hot pressing. Compared with the ceramic composite without  $\text{CaF}_2$ , the results concluded that the mechanical properties of ceramics were improved, the flexural strength, hardness and fracture toughness reached a higher maximum and in addition the main cutting force and cutting temperature were reduced by 13.2% and 26.9%, respectively.

The future challenge from this final work of Master is to evaluate the elaboration of ceramic tiles with addition of wastes from step 1 of the neutralization process, since it is necessary to study the mechanical strength, the setting time, the water absorption and other properties of the ceramic tiles taking into account the European standard EN 197-1:2011.

The valorization of calcium fluoride in ceramic tiles can be achieved through its incorporation into a composition of red stoneware which is the raw material used for the standard ceramic tiles. Additionally, several mixtures with red stoneware (RSM) and different concentrations of  $\text{CaF}_2$  sludge (3%, 5%, 7%, 10%, 30% and 50%) should be tested, for the measurement of properties as apparent porosity and the bulk density according to ASTM C373-88, water absorption according to EN ISO 10545-3, and bending strength according to EN 843, in order to compare with a commercial standard ceramic tile.

Although the investigation group has previously evaluated the incorporation of phosphogypsum on the technical, mechanical and environmental properties of cement mortars, the novelty is to make a study with the wastes obtained. The innovative future study is the replacement of part of the proportion of sludge from Ordinary Portland cement (OPC) in the clinker heating with the obtained waste from step 1, and comparing with commercial cement type I 52.5 N, as the 55% of the waste is fluorite. The study needs to be conducted with different percentages, 2%, 4%, 6%, 8% and 10% of fluorite in the mixing sludge and could be really interesting from economical and technical point of view.





In addition, from the new cements created by waste addition, it could be made concretes and evaluate the following tests: absorption and density (EN-12390-7), consistency (UNE-EN 12350-2), splitting test (UNE-EN 12390-6), modulus of elasticity (UNE-EN 83316) and shrinkage (ASTM C157).

### 3.4.2 Hydroxyapatite

Water soluble fertilizers are the main P source used worldwide. They play an essential role in agriculture because they enable fast increase in P available in soil solution and in P bioavailability (Bolan et al., 2003). The phosphate mineral, mainly of the apatite group, is found in the nature mixed with a wide variety of impurities such as clay, silica, calcite, dolomite, organic matter and various other inorganic compounds. These impurities have an adverse effect in the manufacture of phosphoric acid, so they must be reduced to the lowest possible level (Al-Fariss et al, 1992). There are different methods to achieve an efficient separation of the impurities. Clay usually can be separated by washing or scrubbing, but there are also methods more sophisticated to separate silica, calcite and dolomite such as flotation or calcination.

In the case of the second solid waste, the calcium phosphate is already cleaned because the neutralization process has been applied and the most of contaminants are eliminated as it was discussed in the previous chapters. In the **Table 10** is shown a comparison between the compositions of many phosphate rocks used to produce phosphoric acid in different parts of the world. As it can be seen in the table, the waste obtained contains in the order of Marruecos phosphorite of silicium dioxide ( $\text{SiO}_2$ ), in order of 5 times less of aluminium oxide ( $\text{Al}_2\text{O}_3$ ) than Brasil carbonatite and a hundred times less of ferrum oxide ( $\text{Fe}_2\text{O}_3$ ). Moreover, the hydroxyapatite (HA) obtained has 200 times less of F than Venezuela phosphate rock, which is the rock with less F content. Regarding with the content of Ca and P, the waste has calcium concentration similar to Peru phosphorite and P content in proportions near Venezuela phosphate rocks. The HA of this study contents more MgO than Florida and Marruecos phosphate rock, and also Peru and Venezuela but it has less than Brasil phosphorite and carbonatite.

Nothold et al, (1989) divides exploitable phosphorus deposits into three types: (1) *sedimentary rocks marine or phosphorite rocks*, such as those from the Cretaceous-Eocene of North Africa and Middle East and those of the Miocene of the SE United States; (2) *igneous rocks*, particularly carbonatites and other alkaline rocks such as those from the Kola Peninsula in NW Russia, Goiás and São Paulo in Brazil, and Palabora in South Africa; (3) *insular deposits* such as those of the tropical islands of the Pacific and Indian Ocean. Of all of them, 80% of what is exploited comes from phosphorites (Glenn et al, 1994).



The study of trace elements is extremely important, from two points of view; on the one hand to evaluate their economy as by-products (U and Rare Earths) in the exploitation of phosphates and on the other to control its toxicity (Cd, radionuclides derivatives of uranium) and the consequent influence on the environment both in fertilizers and in the formation of phosphogypsum (Jarvis et al., 1994).

	Florida (Phosphorite)	Marruecos (Phosphorite)	Brasil (Phosphorite)	Peru (Phosphorite)	Venezuela (Phosphorite)	Brasil (Carbonatite)	HA waste (This study)
SiO <sub>2</sub>	11.2	2.1	33.7	3.2	36	0.6	2.4
Al <sub>2</sub> O <sub>3</sub>	1.8	0.6	8.7		0.3	0.1	0.02
Fe <sub>2</sub> O <sub>3</sub>	0.79	0.23	3.3			6.1	0.06
MgO	0.3	0.4	24.4	0.5	0.1	5.5	2.3
CaO	43.6	51.8	20.2	46.5	38.3	44.3	43.3
P <sub>2</sub> O <sub>5</sub>	30.2	32.9		30.2	25-30	5.3	29.8
CO <sub>2</sub>	nd	5.1		4.4			
F	3.2	4.04		2.9	2		0.01

**Table 10:** Comparison of the chemical composition of phosphate rocks from different deposits around the world. Jarvis et al. (1994); Damasceno (1989); Mc. Clellan (1989); Born (1989).

While some phosphate rocks (soluble phosphorites) can be used without any process, that is, for direct application, the vast majority must be previously treated. The main reason of this is the solubility of apatite group, which is strongly related to the degree of substitution by CO<sub>2</sub> and the size of the grain.

The strategic importance for phosphate rock is attributed to the fact that it is the raw material for the manufacture of phosphate fertilizers, through its main product: phosphoric acid. Beyond phosphoric acid can be done in several ways, the most common method is the one where the phosphate rock is reacted with sulfuric acid by the wet route.

The most widespread phosphate fertilizers are mainly ammonium phosphates (mono and di ammonium) and triple superphosphate. Other fertilizers can be derived, such as ammonium polyphosphates, ammonium phosphate sulfates, and others used minority. Simple superphosphate (SSP) comes from the treatment of phosphate rock with sulfuric acid, and it has been for decades the main phosphate fertilizer although it was displaced from the market due to its low concentration of phosphorus, but recently it has received a greater demand for its contribution of sulfur, which has been revalued as a nutrient. Other phosphate fertilizers can be obtained by reacting the rock with different acids such as nitric (nitrophosphates) or hydrochloric.



The most common practice of SSP production is mixing ground phosphate rock with pure or diluted sulfuric acid. After allowing the reaction progresses throughout the mass of ore (cured), the product can be used directly once it has dried, be granulated for direct use, or be used as an ingredient in fertilizers complex. The main process variables for producing SSP include the fineness of grind of the rock, the concentration of sulfuric acid, the acid-rock ratio and the composition of the phosphoric rock.

P-fertilization can be applied to cropped soil through two main ways, namely: by using soluble phosphates to increase P pools, rapid release and uptake by plants or by using less soluble rock phosphate powder to trigger synchronization between P solubilization and its uptake by plants. A. Somavilla et al (2021) have evaluated whether there is no dissolution of P-bearing minerals in the long-term when phosphate rock is used, as well as to analyze its response associated with P-legacy and plant dry-matter production in comparison to that of fertilization based on soluble phosphate added with limestone. They concluded that the use of soluble P source and limestone resulted in greater nutrient use efficiency and in higher dry matter yield (22 %). In addition, the use of phosphate rock has led to higher total P and moderate-lability P levels in the soil due to low apatite dissolution (even under favorable soil thermodynamics conditions). P-apatite minerals were found in sand and silt soil fractions subjected to phosphate rock treatment, which presented up to 6-year P dissolution and promoted low P bioavailability. Agronomic use of soluble phosphate added with limestone is the most suitable technique used to increase grassland yield and P-use efficiency.

In relation to the second waste, the valorization of calcium phosphate shall be following, although on a lesser scale, the same treatment used by the phosphate industry. The novelty of future studies will be the evaluation of the applicability of the waste as a direct fertilizer and, on the other hand, to digest this waste with sulfuric acid to make new phosphoric acid, since the hydroxyapatite obtained is cleaned from the most of heavy metals such as Fe, Al, and Si. Additionally, the interesting point is that the HA has really low F content, which is consider as a residue in the manufacture process of phosphoric acid.

In both cases, the valorization of the waste must follow the Royal Decree 506/2013 of 28 June 2013 on fertilizer products, which contains seven annexes detailing the technical specifications and other requirements which such products must meet in order to be suitable for use in Spanish agriculture and gardening. Concretely, in the Annex V provides the applicable criteria to fertilizer products made by valorization wastes, such as the limits for heavy metals.



## 4 CONCLUSIONS

The main conclusions and findings found in this work are shown in this section:

1. A sequential neutralization cleaning process of PG leachates in 2 steps with alkaline reagents ( $\text{Ca}(\text{OH})_2$  and  $\text{CaCO}_3$ ) has been optimized.
2. A deep characterization of the NORM wastes obtained in the cleaning process has been conducted and additionally, the environmental impact was evaluated, in relation to final effluents and solid wastes.
3. In this work, has been demonstrated that a sequential neutralization process in two selected steps (at  $\text{pH} = 3.6$  and  $12$ ) is effective in the reduction of contaminants such as heavy metals, anions and radionuclides. Besides, the final concentration of contaminants obtained in the liquid set up all the requirements for discharge into coastal waters, except for the  $\text{pH}$ , which need to be until  $9$ . This fact needs to be studied in deep in future research.
4. A concentration reduction of some of the metals in study, such as Al, Cd, Cr, Cu, Fe, Zn and Pb, in the first step of the sequential process is achieved, since their concentration in the liquid waste is lower than the concentration of those elements in the original phosphogypsum leachate (PGL). Additionally, in step 2 of both processes most of the elements reach concentrations lower than the detection limit of the technique, which means that they have been practically eliminated.
5. The activity concentration obtained of  $^{210}\text{Po}$  and  $^{234-238}\text{U}$  are similar to those found in seawater and it is remarkable that with  $\text{Ca}(\text{OH})_2$  there is a higher efficiency in the removal of radionuclides, since it allows to obtain reductions in concentrations up to  $95\%$ , while with  $\text{CaCO}_3$  it is achieved only  $85\%$ .
6. In relation with the solids obtained in the neutralization process, it is formed fluorite ( $\text{CaF}_2$ ) in the first step of neutralization with  $\text{CaCO}_3$ , while with  $\text{Ca}(\text{OH})_2$  it is formed a lower quantity of fluorite, gypsum ( $\text{CaSO}_4 \cdot 2\text{H}_2\text{O}$ ), brushite ( $\text{CaHPO}_4 \cdot 2\text{H}_2\text{O}$ ) and ardealite ( $\text{Ca}_2(\text{SO}_4)(\text{HPO}_4) \cdot 4\text{H}_2\text{O}$ ).
7. Regarding with the solids obtained in the second phase, which corresponds to Hydroxylapatite ( $\text{Ca}_5(\text{PO}_4)_3\text{OH}$ ), it is significant that with  $\text{Ca}(\text{OH})_2$  the quantity of HA is lower and the impurities of the solid are conformed by a major content of As, Ni and Sr.
8. Additionally, the approach of making two processes with different reagents was made in order to compare them. One readable point is the higher precipitation of some elements such as As, Cd, Ni, P, S, Si, Sr and U with  $\text{Ca}(\text{OH})_2$  comparing with  $\text{CaCO}_3$ , but on the other hand, the most interest



result is that with  $\text{CaCO}_3$ , it is possible to obtain an As concentration 75% lower than in the case of neutralization with  $\text{Ca(OH)}_2$ . The other elements are in the same order in both processes and after the leaching test, they could be classified as Inert Waste, with exception of the content of Cd, in which case need to be classified as No Hazardous waste.

9. This differentiation enhances the possibility to makes studies with specific objectives, since it is possible to make a first step of neutralization with  $\text{CaCO}_3$  for obtaining a solid waste with less As and evaluate the possibilities of their valorisation in the context of circular economy. Moreover, in the case of  $\text{Ca(OH)}_2$  process, the generated waste cannot be disposed in a landfill, since it outpoints the limit for hazardous waste for As. In that case, it is necessary additional research to determine the behavior of this contaminant and final disposal.
10. It is possible to reuse the solids of step 1 in the industry of cement, as a mineral addition, and in the elaboration of ceramics. In this case, everything suggests that it is better to use  $\text{CaCO}_3$  in the neutralization first step, since it is possible to obtain a more purity waste. The future study in deep of the application options is an interesting topic, in order to obtain the best formulation in terms of technical properties and economic implications for its use in the manufacture of cement and ceramics.
11. In relation with the second solid, the importance is to obtain a high purity waste because of the reuse options, which are the possibilities to use it in the fertilizer industry, reusing the cleaned compounds of calcium phosphates in their digestion with sulfuric acid to obtain new phosphoric acid. This is another future study which seems to be interesting.



## 5 REFERENCES

Akın Altun (1999). Effect of CaF<sub>2</sub> and MgO on sintering of cement Clinker. *Cement and Concrete Research* 29 (1999) 1847–1850.

Andre Somavilla, Laurent Caner, Edson Campanhola Bortoluzzi, Maria Alice Santanna, Danilo Rheinheimer dos Santos (2021). P-legacy effect of soluble fertilizer added with limestone and phosphate rock on grassland soil in subtropical climate region. *Soil & Tillage Research* 211 (2021) 105021.

Anne P. M. Velenturf, Phil Purnell. Principles for a sustainable economy. *Sustainable Production and Consumption* 27 (2021) 1437–1457.  
<https://doi.org/10.1016/j.spc.2021.02.018>

Bolan, N.S., Adriano, D.C., Naidu, R., 2003. Role of phosphorus in (Im)mobilization and bioavailability of heavy metals in the soil-plant system. *Reviews of Environmental Contamination and Toxicology*. Springer, New York.  
[https://doi.org/10.1007/0-387-21725-8\\_1](https://doi.org/10.1007/0-387-21725-8_1), p. 177.

Bolívar J.P., García-Tenorio R. and García-León M. On the fractionation of natural radioactivity in the production of phosphoric acid by the wet acid method. *J. Radioanalytical Nuclear Chemistry Letters* 214 (1996) 77-88.

Bolívar J.P., García-Tenorio R. y Mas, J.L. Radioactivity of phosphogypsum in the South-West of Spain. *Radiation Protection Dosimetry* 76 (1998) 185-189.

Bolívar, J. P., García-Tenorio, R., Mas, J. L., & Vaca, F. (2002). Radioactive impact in sediments from an estuarine system affected by industrial wastes releases. *Environment International*, 27(8), 639–645.  
[https://doi.org/10.1016/S0160-4120\(01\)00123-4](https://doi.org/10.1016/S0160-4120(01)00123-4)

Bolívar, J. P., Martín, J. E., García-Tenorio, R., Pérez-Moreno, J. P., & Mas, J. L. (2009). Behaviour and fluxes of natural radionuclides in the production process of a phosphoric acid plant. *Applied Radiation and Isotopes*, 67(2), 345–356. <https://doi.org/10.1016/j.apradiso.2008.10.012>

Born, H., 1989. The Jacupiranga apatite deposit, Sao Paulo, Brazil En: Notholt, J., R. Sheldon y D. Davidson (Eds.), *Phosphate rocks resources*, 2(18):111-115. Cambridge

Damasceno. E.C. 1989. The Patos de Minas phosphate deposits, Minas Gerais, Brazil En: Notholt, J., R. Sheldon y D. Davidson (Eds.), *Phosphate rocks resources*, 2(16) 100-103. Cambridge.

Dandan Feng, Yumei Zhu, Fengfeng Li, Zhihong Li (2016). Influence investigation of CaF<sub>2</sub> on the L-A-S based glass-ceramics and the glass-ceramic/diamond composites. *Journal of the European Ceramic Society* 36 (2016) 2579–2585.





Decreto 109/2015, de 17 de marzo, por el que se aprueba el Reglamento de Vertidos al Dominio Público Hidráulico y al Dominio Público Marítimo-Terrestre de Andalucía (BOJA nº 89 de 12/05/2015).

Directiva 2008/98/CE del Parlamento Europeo y del Consejo, de 19 de noviembre de 2008, sobre los residuos y por la que se derogan determinadas Directivas. «DOUE» núm. 312, de 22 de noviembre de 2008, páginas 3 a 30 (28 págs.). Departamento: Unión Europea. Referencia: DOUE-L-2008-82319.

Ed. N.G. Maldonado, M.F. Carrasco. “Ese material llamado hormigón”. Asociación Argentina de Tecnología del Hormigón. 2012

EN 12390-7, Test Method for Density, Relative Density (Specific Gravity), and Absorption of Fine Aggregate.

EN ISO 10545-3:2018 Ceramic tiles - Part 3: Determination of water absorption, apparent porosity, apparent relative density and bulk density.

Environmental Protection Agency of United States (US, EPA, 2012). <https://www.epa.gov/>

EU Council Directive 2013/59/Euratom of 5 December 2013 laying down basic safety standards for protection against the dangers arising from exposure to ionising radiation.

European standard EN 196- 3:2009 (Methods of testing cement - Part 3: Determination of setting times and soundness).

European standard EN 197-1:2011 - Cement - Part 1: Composition, specifications and conformity criteria for common cement.

FAO. 2019. World fertilizer trends and outlook to 2022. Rome. ISBN 978-92-5-131894-2. <https://www.fao.org/3/ca6746en/ca6746en.pdf>

FAO-IFA. (2019). Executive Summary Fertilizer Outlook 2019-2023. IFA Annual Conference, June, 26–28. [file:///C:/Users/3PX67LA\\_RS5/Downloads/2019\\_IFA\\_Annual\\_Conference\\_Montreal\\_Fertilizer\\_Outlook\\_2019-2023\\_Summary.pdf](file:///C:/Users/3PX67LA_RS5/Downloads/2019_IFA_Annual_Conference_Montreal_Fertilizer_Outlook_2019-2023_Summary.pdf)

Glenn, C.R., Föllmi, K.B., Riggs, S.R., Baturin, G.N., Grimm, K.A., Trappe, J., Abed, A.M., Galli-Olivier, C., Garrison, R.E., Ilyin, A.V., Jehl, C., Rohrlich, V., Sadaqah, R.M., Schidlowski, M., Sheldon, R.E. y Siegmund, H., 1994. Phosphorous and phosphorites: sedimentology and environments of formation. Journal of Swiss Geological Society, Eclogae Geologica Helvetica 87: 747-788. Zurich, Suiza.

Guerrero J.L., Gutiérrez-Álvarez I., Mosqueda F., Olías M., García-Tenorio R., and Bolívar J.P. Pollution evaluation on the saltmarshes under the phosphogypsum stacks of Huelva due to deep leachates. Chemosphere 230 (2019) 219-229.





Guerrero, J. L., Perez-Moreno, S. M., Gutierrez- Alvarez, I., Gazquez, M. J., & Bolívar, J. P. (2020). Behaviour of heavy metals and natural radionuclides in the mixing of phosphogypsum leachates with seawater (ARTICLE IN PRESS). *Environmental Pollution*. <https://doi.org/10.1016/j.envpol.2020.115843>

Heffer, P. and Prudhomme, M., 2016. Fertilizer outlook 2016-2020. 84th IFA AnnualConference Moscow (Russia), Junio 2016, 7pp.

Humphries, M. S., McCarthy, T. S., and Pillay, L. Attenuation of pollution arising from acid mine drainage by a natural wetland on the Witwatersrand. *South African Journal of Science* 113 (2017) 1-9.

IAEA/AQ/17. IAEA Analytical Quality in Nuclear Applications Series No. 17

International Fertilizer Industry Association (IFA), Phosphate rock statistics; trends from 1992 to 2011 (2011).

International Phosphogypsum Working Group, PGWG.  
<http://www.pgwg.stackfree.com/Home.aspx>

Jarvis, I., Burnett, W., Nathan, J., Almayaydin, F., Attia, A., Castro L., Husain, V.; Qutawna, A. y Zanin Y., 1994. Phosphorites geochemistry. State of the art environmental concern. *Eclogae Geologiae Helvetiae Journal of Swiss Geologicae Society*. 87(3): 643-700. Zurich, Suiza. Johnston, A.E. 2000. Soil and Plant Phosphate. International Fertilizer Industry Association. Paris,

Jianping Wang, Mingdong Yi, Chonghai Xu, Guangchun Xiao, Zhaoqiang Chen, Jingjie Zhang, Li Wang. Mechanical property and cutting performance of (W,Ti) C based ceramic composites with the addition of nano-sized CaF<sub>2</sub>. *International Journal of Refractory Metals and Hard Materials* 99 (2021) 105607.

Jones S. N., and Cetin B. Evaluation of waste materials for acid mine drainage remediation. *Fuel* 188 (2017) 294–309.

Kefeni K. K., Msagati T. A.M., and Mamba B. B. Acid mine drainage: Prevention, treatment options, and resource recovery: A review. *Journal of Cleaner Production* 151 (2017) 475-493.

Ley 7/2022, de 8 de abril, de residuos y suelos contaminados para una economía circular. [BOE-A-2022-5809](https://www.boe.es/eli/es/l/2022/04/08/7/con).  
<https://www.boe.es/eli/es/l/2022/04/08/7/con>

McClellan, G.H.. 1989. Geology of the phosphate deposits ay Sechura, Peru En: Notholt, J., R. Sheldon y D. Davidson (Eds.), *Phosphate rocks resources*, 2(16) :124-130. Cambridge.

Mohammed Dahhou, Adnane El Hamidi, Mohammed El Moussaouiti, Muhammad Azeem Arshad, (2021). Synthesis and characterization of belite



clinker by sustainable utilization of alumina sludge and natural fluorite (CaF<sub>2</sub>). *Materialia* 20 (2021) 101204.

Millán-Becerro R., Pérez-López R., Macías F., Cánovas C.R., Papaslioti E.M. and Basallote. M.D. Assessment of metals mobility during the alkaline treatment of highly acid phosphogypsum leachates. *Science of the Total Environment* 660 (2019) 395–405.

Nleya, Y., Simate, G. S. and Ndlovu, S. Sustainability assessment of the recovery and utilization of acid from acid mine drainage. *Journal of Cleaner Production* 113 (2016) 17 27.

Notholt, A.J.G., Sheldon, R.P. y Davidson, D.F., 1989. Phosphate rock resources, Phosphate deposits of the world. Cambridge University Press, Cambridge.

O. Dominguez, A. Torres-Castillo, L.M. Flores-Veleza, R. Torresc (2010). Characterization using thermomechanical and differential thermal analysis of the sinterization of Portland clinker doped with CaF<sub>2</sub>. *Materials characterization* 61 (2010) 459 – 466.

Papaslioti, E. M., Pérez-López, R., Parviainen, A., Sarmiento, A. M., Nieto, J. M., Claudio Marchesia, A., & Delgado-Huertasa, C. J. (2018). Effects of seawater mixing on the mobility of trace elements in acid phosphogypsum leachates. *Marine Pollution Bulletin*, 127, 695–703.  
<https://doi.org/10.1016/j.marpolbul.2018.01.001>

Pérez-López R., Macías F., Ruiz Cánovas C., Miguel Sarmiento A., and Pérez-Moreno S. M. Pollutant flows from a phosphogypsum disposal area to an estuarine environment: An insight from geochemical signatures. *Science of the Total Environment* 553 (2016) 42–51.

Pérez-López, R., Macías, F., Cánovas, C. R., Sarmiento, A. M., & Pérez-Moreno, S. M. (2016a). Pollutant flows from a phosphogypsum disposal area to an estuarine environment: An insight from geochemical signatures. *Science of the Total Environment*, 553, 42–51. <https://doi.org/10.1016/j.scitotenv.2016.02.070>

Pérez-López, R., Macías, F., Cánovas, C. R., Sarmiento, A. M., & Pérez-Moreno, S. M. (2016b). Pollutant flows from a phosphogypsum disposal area to an estuarine environment: An insight from geochemical signatures. *Science of the Total Environment*, 553, 42–51. <https://doi.org/10.1016/j.scitotenv.2016.02.070>

Periáñez, R., Hierro, A., Bolívar, J. P., & Vaca, F. (2013). The geochemical behavior of natural radionuclides in coastal waters: A modeling study for the Huelva estuary. *Journal of Marine Systems*, 126, 82–93.  
<https://doi.org/10.1016/j.jmarsys.2012.08.001>



Real Decreto 506/2013, de 28 de junio, sobre productos fertilizantes. «BOE» núm. 164, de 10/07/2013. Referencia:BOE-A-2013-7540Permalink ELI: <https://www.boe.es/eli/es/rd/2013/06/28/506/con>.

Real Decreto 646/2020, de 7 de julio, por el que se regula la eliminación de residuos mediante depósito en vertedero. Ministerio para la Transición Ecológica y el Reto Demográfico.

Reference Material IAEA 434:Naturally Occurring Radionuclides in Phosphogypsum. Referencia: BOE-A-2020-7438.September 2000.

Rudnick et Gao, "Composition of the Continental Crust", Treatise of Geochemistry. Elsevier, vol. 3, The crust, 2003, pp. 1-64.

T.F. Al-Fariss, H.O. Ozbelge and H.S. El-Shall (1992). On the Phosphate Rock Beneficiation for the Production of Phosphoric Acid in Saudi Arabia. J. King Saud Univ., Vol. 4, Eng. Sci. (1), pp. 13-32 (1412 A.H.1992)

Taylor T.J., Pape S., and Murphy N. A (2005) Summary of Passive and Active Treatment Technologies for Acid and Metalliferous Drainage (AMD). Fifth Australian Workshop on Acid Drainage 29-31 August 2005, Fremantle, Australia. Australian Business Number 29006227532.

TRAGSATEC (2011). Diagnose for stablishing the project for remediation the phosphogypsum piles located at Huelva (Spain) (In Spanish).

UNE-EN 12350-2:2009. Testing fresh concrete - Part 2: Slump-test.

UNE-EN 12390-6:2010 Testing hardened concrete - Part 6: Tensile splitting strength of test specimens.

UNE-EN 12457. Characterization of waste Leaching Compliance test for leaching of granular waste materials and sludges (2003).

UNE-EN 196-1, 2018. Methods of testing cement - Part 1: Determination of strength.

UNE-EN 480-5, 2006. Admixtures for Concrete, Mortar and Grout. Test Methods. Part 5: Determination of Capillary Absorption.

UNE-EN 83316: 1996 Concrete tests. Determination of the modulus of elasticity in compression.

UNE-EN 843-6:2009 Advanced technical ceramics - Mechanical properties of monolithic ceramics at room temperature - Part 6: Guidance for fractographic investigation.

UNSCEAR. (2000). Sources and Effects of Ionizing Radiation, United Nations Scientific Committee on the Effects of Atomic Radiation UNSCEAR 2000



**TFM – MTA**

*Characterization and valorization diagnosis of generated wastes in the decontamination process of Phosphogypsum Leachate*

Report to the General Assembly, with Scientific Annexes. In UNSCEAR 2000 Report: Vol. I.

USGS (U.S. Geological Survey), 2017. Mineral commodity summaries 2017. U.S. Geological Survey, 202pp.

V. Bonavetti. Tesis de Magister en Tecnología y construcciones de Hormigón “Cementos con filler calcáreo. Mecanismo de interacción y su influencia sobre las propiedades resistentes”. Universidad del Centro de la Provincia de Buenos Aires, Olavarría, Argentina, 1998.

Wei-Ting Lin (2019). Characterization and permeability of cement-based materials containing calcium fluoride sludge. *Construction and Building Materials* 196 (2019) 564–573.



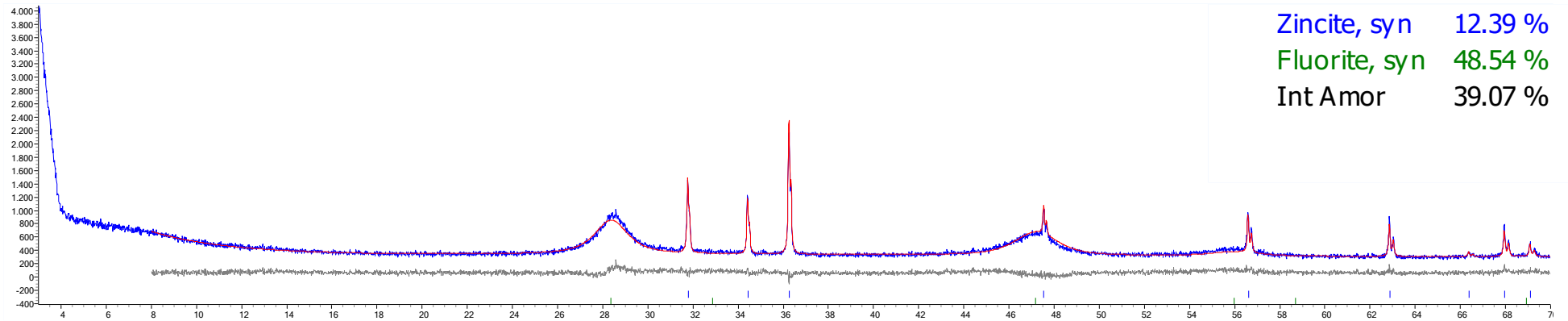
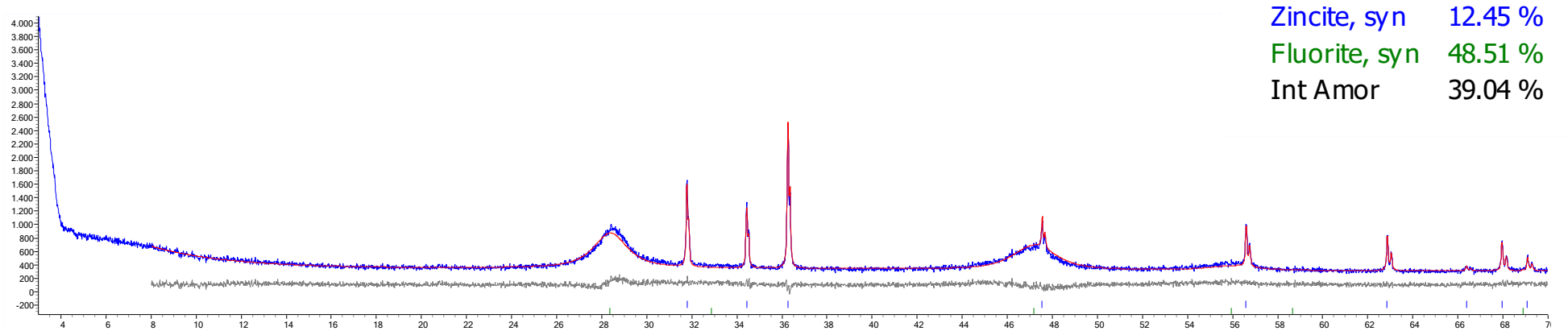
## 6 ANEXXES

### 6.1 Composition (mg/L) of PGL and liquid fraction measured by ICP-OES and ICP-MS.

Parameters	Liquid fraction				
	PGL	Process A		Process B	
		LA1	LA2	LB1	LB2
pH	1.7	3.5	12	3.5	12
EC (mS/cm)	30.2	24.3	19.1	23.8	18.7
Eh (mV)	656	557	163	553	177
Element	C (mg/L)	C (mg/L)	C (mg/L)	C (mg/L)	C (mg/L)
Al	6.5	0.9	0.3	0.9	0.3
As	27.4	26.5	<0,1	26.1	<0,1
Ca	1660	4700	213	3900	180
Cd	7.8	7.3	<0,1	7.0	<0,1
Cr	22.1	3.6	<0,1	2.0	<0,1
Cu	8.7	5.3	0.1	4.6	0.1
Fe	129	0.7	<0,1	0.3	<0,1
K	268	252	227	251	204
Mg	906	875	0.7	886	<0,1
Mn	12.4	12.5	<0,1	12.7	<0,1
Na	4920	4880	4030	4800	4020
Ni	5.6	5.4	0.2	5.0	0.2
P	10900	8900	8.7	8460	5.7
Pb	0.8	<0,1	<0,1	<0,1	<0,1
S	1510	1440	236	1090	184
Si	512	463	4.1	445	4.3
Sr	47.0	38.8	1.3	36.8	1.1
U	20.5	3.6	<0,1	0.8	<0,1
Zn	65.9	45.6	<0,1	38.6	<0,1



## 6.2 Diffraction patterns of solid fraction formed after neutralization treatment measured by XRD.

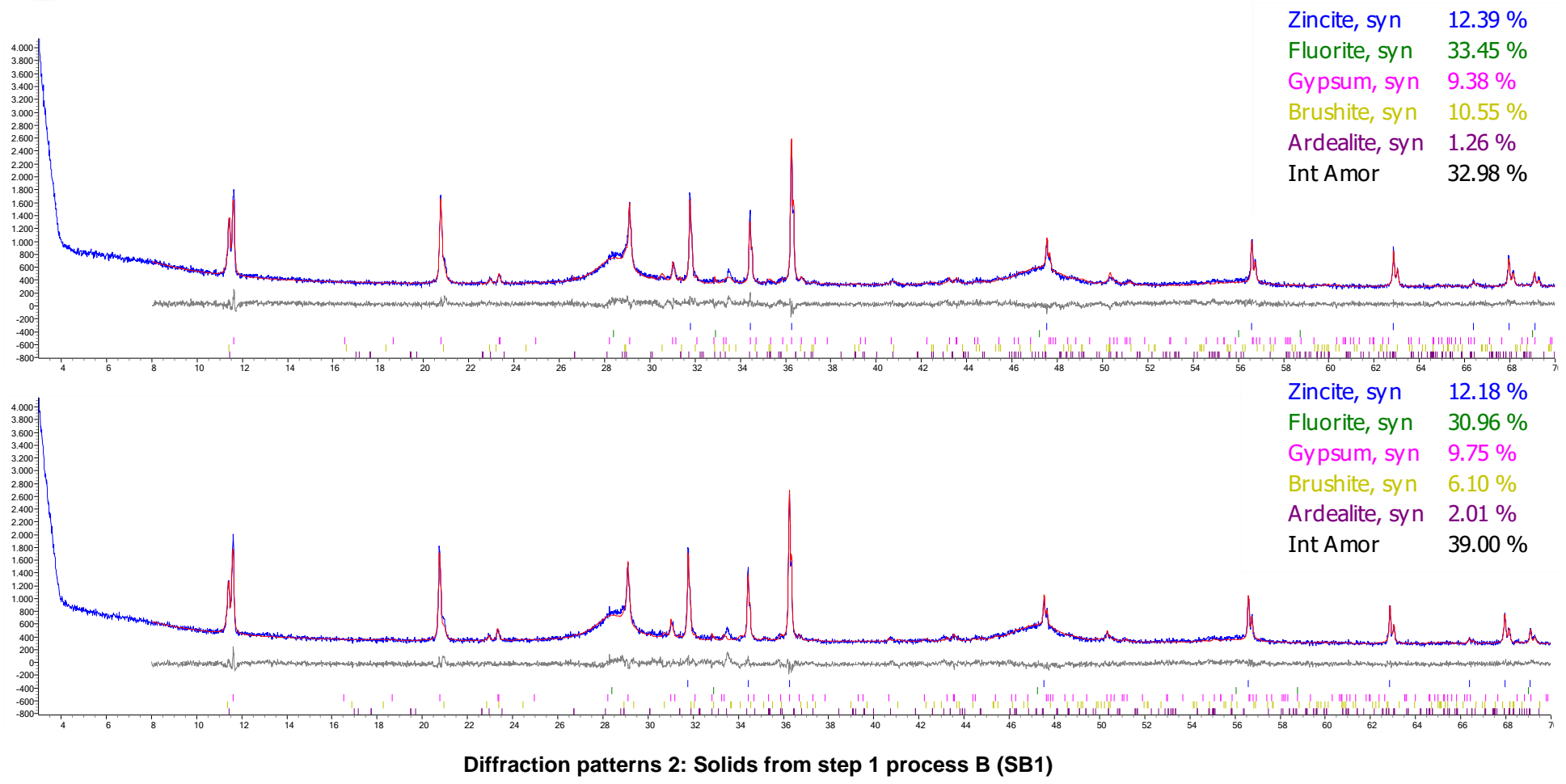


Diffraction patterns 1: Solids from step 1 process A (SA1)



**TFM – MTA**

*Characterization and valorization diagnosis of generated wastes in the decontamination process of Phosphogypsum Leachate*

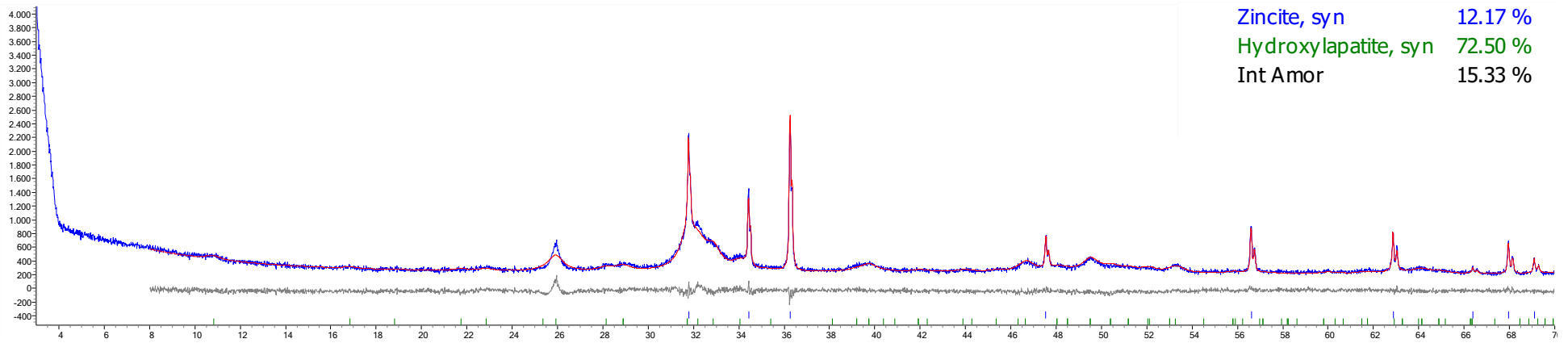
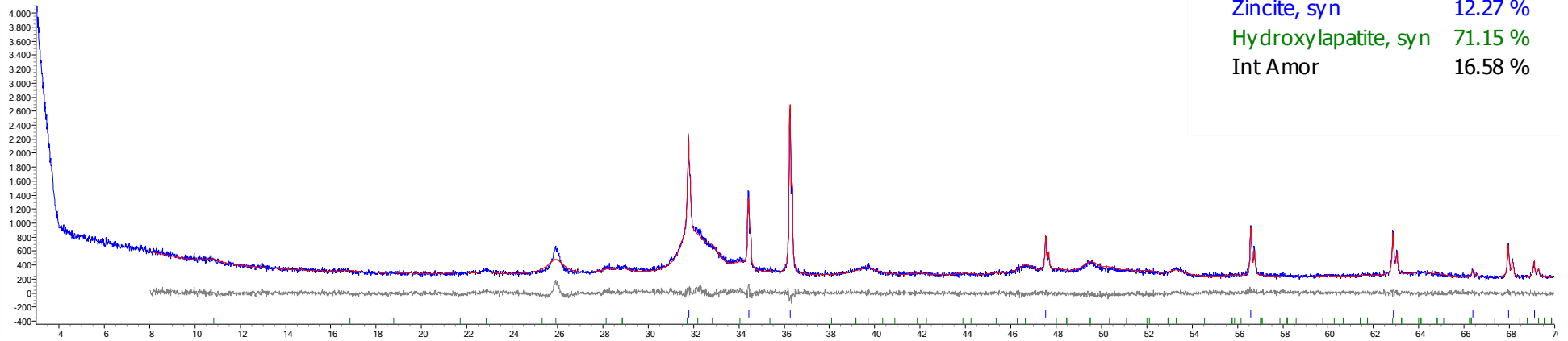




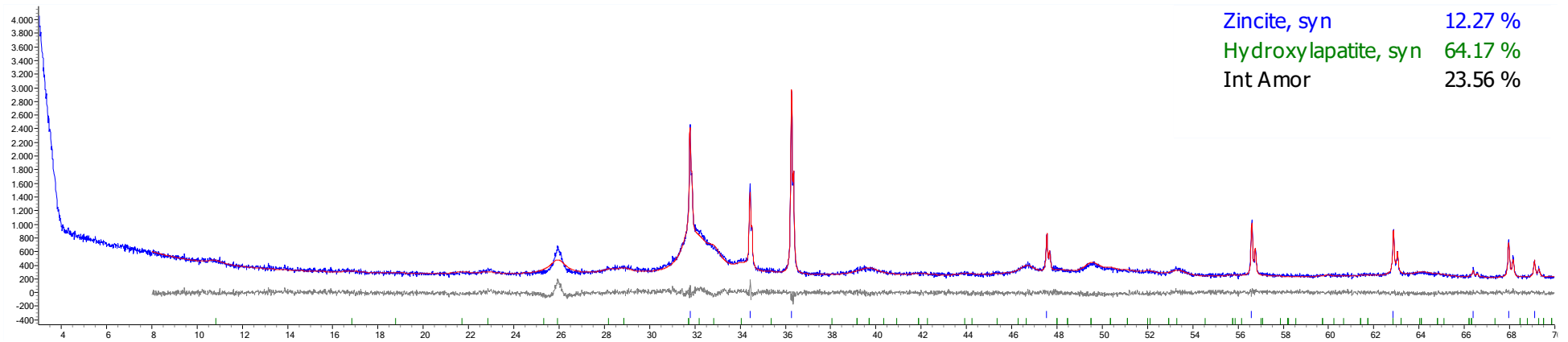
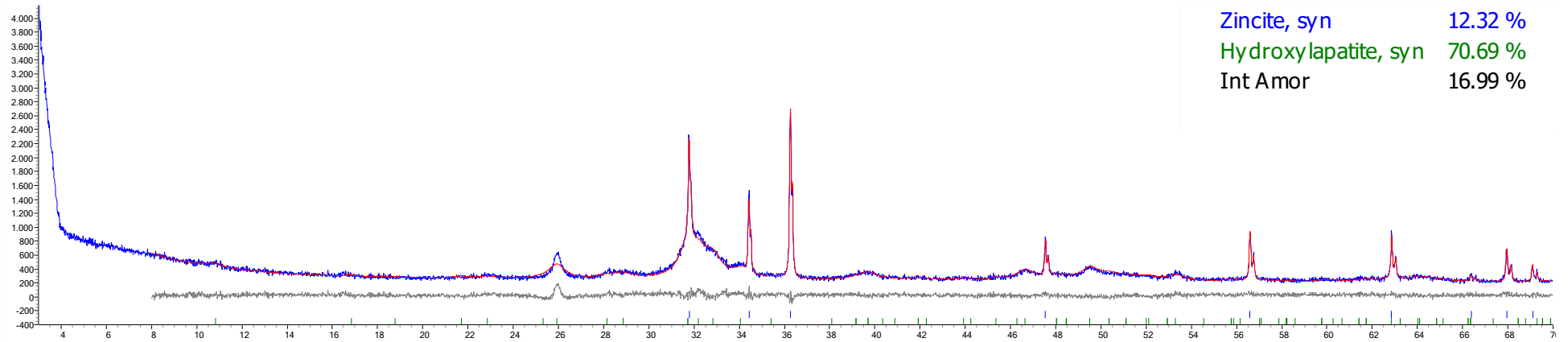


**TFM – MTA**

*Characterization and valorization diagnosis of generated wastes in the decontamination process of Phosphogypsum Leachate*



**Diffraction patterns 3: Solids from step 2 process A (SA2)**



Diffraction patterns 4: Solids from step 2 process B (SB2)



### 6.3 Mineral composition of solid fraction formed after neutralization treatment measured by XRD.

Compound	Solid fraction			
	SA1	SA2	SB1	SB2
	Nominal percentage	Nominal percentage	Nominal percentage	Nominal percentage
<i>Zincite (internal pattern)</i>	12.4	12.2	12.3	12.3
Amorphous content	44.6±0.9	18.2±0.8	41.0±0.1	23.2±0.6
(Ca <sub>5</sub> (PO <sub>4</sub> ) <sub>3</sub> OH) Hydroxylapatite		81.8±0.7		76.9±0.6
(CaF <sub>2</sub> )Fluorite	55.4±0.9		36.8±0.9	
(CaSO <sub>4</sub> ·2H <sub>2</sub> O) Gypsum			10.9±0.5	
(Ca <sub>2</sub> (SO <sub>4</sub> )(HPO <sub>4</sub> )·4H <sub>2</sub> O) Ardealite			1.9±0.4	
(CaHPO <sub>4</sub> ·2H <sub>2</sub> O) Brushite			9.5±0.6	



## 6.4 Elemental composition (% and ppm) of solid fraction formed after neutralization treatment measured by ICP-MS and XRF.

Solid fraction				
Element	Process A		Process B	
	SA1	SA2	SB1	SB2
<b>Major elements</b>				
Al (%)	0.1	0.01	0.1	0.01
Ca (%)	26.5	31.3	25.7	30.5
F (%)	18.8	<0.01	13.6	<0.01
Fe (%)	1.6	0.04	1.3	0.04
K (%)	0.2	0.1	0.1	0.2
Mg (%)	0.5	1.4	0.3	1.4
Na (%)	0.7	2.4	0.3	2.3
P (%)	7.2	12.4	6.7	13.6
S (%)	0.5	2.3	3.2	1.8
Si (%)	0.02	1.1	0.02	1.1
Zn (%)	0.2	0.1	0.2	0.1
<b>Minor elements</b>				
Cd (ppm)	71.7	141.5	65.5	154
As (ppm)	133	465	95.3	517.5
Cr (ppm)	2115	58.5	1680	29
Cu (ppm)	457.5	72.6	385.5	72.1
Mn (ppm)	118	222.5	119	232
Ni (ppm)	5.9	83.3	2.6	97.0
Pb (ppm)	44.1	<0,5	66.4	<0,5
Sr (ppm)	>1000	509	>1000	553.5
U (ppm)	1820	49.8	1500	13.5



## 6.5 Material balances - Composition of liquid and solid fraction during neutralization treatment (Process A).

Element	Process A							
	Vo liq (mg)	V1 liq (mg)	m1 solid (mg)	Error	V1 liq (mg)	V2 liq (mg)	m2 solid (mg)	Error
Al	13.0	1.7	16.4	39%	1.7	0.4	10.8	85%
As	55.0	50.2	2.1	5%	50.2	0.1	50.3	0.4%
Ca	3327.4	8906.5	4918.8	30%	8906.5	301.7	35940.7	19%
Cd	15.7	13.8	1.1	5%	13.8	0.1	15.3	10%
Cr	44.3	6.8	33.1	10%	6.8	0.1	6.3	7%
Cu	17.4	10.0	7.2	1%	10.0	0.1	7.9	26%
Fe	258.6	1.3	250.6	3%	1.3	0.1	43.3	97%
K	536.8	477.7	25.1	6%	477.7	321.8	129.9	6%
Mg	1816.4	1658.9	91.6	4%	1658.9	1.0	1580.5	5%
Mn	24.8	23.7	1.8	3%	23.7	0.1	24.1	2%
Na	9861.9	9247.6	98.7	5%	9247.6	5702.5	2067.7	19%
Ni	11.2	10.2	0.1	8%	10.2	0.3	9.0	10%
P	21848.6	16865.5	1347.2	17%	16865.5	12.3	13423.6	26%
Pb	1.5	0.1	0.7	49%	0.1	0.1	0.0	3%
S	3027.3	2728.8	76.8	7%	2728.8	333.4	2489.9	3%
Sr	94.3	73.5	12.5	9%	73.5	1.8	55.1	29%
Zn	132.1	86.4	39.9	4%	86.4	0.1	73.2	18%
Si	1027.3	877.2	3.1	14%	877.2	5.8	21.7	97%
U	41.1	6.8	28.5	14%	6.8	0.1	5.4	25%



## 6.6 Material balances - Composition of liquid and solid fraction during neutralization treatment (Process B).

Element	Process B							
	Vo lix (mg)	V1 liq (mg)	m1 solid (mg)	Error	V1 liq (mg)	V2 liq (mg)	m2 solid (mg)	Error
Al	13.0	1.6	15.4	30%	1.6	0.4	9.9	85%
As	55.0	49.0	2.1	7%	49.0	0.1	51.5	5%
Ca	3326.3	7322.3	6358.0	30%	7322.3	261.6	29536.7	19%
Cd	15.7	13.1	1.4	7%	13.1	0.1	15.3	17%
Cr	44.3	3.8	37.0	8%	3.8	0.1	2.9	21%
Cu	17.4	8.6	8.5	1%	8.6	0.1	7.2	15%
Fe	258.5	0.6	283.8	10%	0.6	0.1	39.8	99%
K	536.7	470.7	24.2	8%	470.7	296.4	149.2	5%
Mg	1815.8	1663.1	64.9	5%	1663.1	0.1	1422.1	14%
Mn	24.7	23.8	2.6	7%	23.8	0.1	23.1	3%
Na	9858.7	9012.0	63.8	8%	9012.0	5829.0	1899.5	14%
Ni	11.2	9.4	0.1	16%	9.4	0.3	9.6	6%
P	21841.5	15883.7	1764.4	19%	15883.7	8.3	13525.2	15%
Pb	1.5	0.1	1.5	2%	0.1	0.1	0.0	4%
S	3026.4	2046.5	704.0	9%	2046.5	266.9	1760.3	1%
Sr	94.2	69.1	14.3	12%	69.1	1.6	55.0	18%
Zn	132.1	72.5	51.5	6%	72.5	0.1	63.6	12%
Si	1026.9	834.7	235.4	4%	834.7	6.2	1074.1	29%
U	41.1	1.5	32.9	16%	1.5	0.1	1.3	6%

## 6.7 Element precipitation percentage during process A and B.



Element	Process A				Process B			
	LA1	SA1	LA2	SA2	LB1	SB1	LB2	SB2
<b>Al</b>	13.1%	86.9%	24.9%	75.1%	12.3%	87.7%	22.7%	77.3%
<b>As</b>	91.3%	8.7%	0.1%	99.9%	89.1%	10.9%	0.1%	99.9%
<b>Ca</b>	62.8%	37.2%	3.4%	96.6%	62.5%	37.5%	3.6%	96.4%
<b>Cd</b>	88.0%	12.0%	0.5%	99.5%	83.7%	16.3%	0.6%	99.4%
<b>Cr</b>	15.4%	84.6%	1.0%	99.0%	8.5%	91.5%	1.9%	98.1%
<b>Cu</b>	57.8%	42.2%	1.4%	98.6%	49.7%	50.3%	1.7%	98.3%
<b>Fe</b>	0.5%	99.5%	5.3%	94.7%	0.2%	99.8%	12.9%	87.1%
<b>K</b>	89.0%	11.0%	67.4%	32.6%	87.7%	12.3%	63.0%	37.0%
<b>Mg</b>	91.3%	8.7%	0.1%	99.9%	91.6%	8.4%	0.0%	100.0%
<b>Mn</b>	95.7%	4.3%	0.3%	99.7%	96.4%	3.6%	0.3%	99.7%
<b>Na</b>	93.8%	6.2%	61.7%	38.3%	91.4%	8.6%	64.7%	35.3%
<b>Ni</b>	91.0%	9.0%	2.8%	97.2%	83.5%	16.5%	3.1%	96.9%
<b>P</b>	77.2%	22.8%	0.1%	99.9%	72.7%	27.3%	0.1%	99.9%
<b>Pb</b>	6.2%	93.8%	74.7%	25.3%	6.1%	93.9%	77.2%	22.8%
<b>S</b>	90.1%	9.9%	12.2%	87.8%	67.6%	32.4%	13.0%	87.0%
<b>Sr</b>	78.0%	22.0%	2.5%	97.5%	73.3%	26.7%	2.3%	97.7%
<b>Zn</b>	65.4%	34.6%	0.1%	99.9%	54.9%	45.1%	0.1%	99.9%
<b>Si</b>	85.4%	14.6%	0.7%	99.3%	81.3%	18.7%	0.7%	99.3%
<b>U</b>	16.6%	83.4%	1.0%	99.0%	3.7%	96.3%	4.8%	95.2%





### 6.8. Composition of reagents used in sequential optimization neutralization process, A and B – measured by ICP-MS.

Code	Reagent	Concentration (ppm)										
		Cr	Mn	Ni	Cu	Zn	As	Sr	Cd	Ba	Pb	U
22-1131	CaCO <sub>3</sub>	318	839	257	833	136	119	1777	4.1	193	36	8.7
22-1132	Ca(OH) <sub>2</sub>	380	2025	331	619	99	189	2708	1.4	109	7.1	2.1